

S2E simulations of THz SASE FEL proof-of-principle experiment at PITZ

Mikhail Krasilnikov

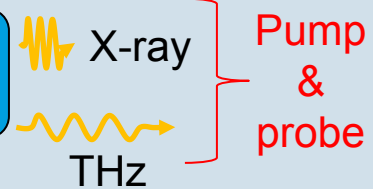
PPS, DESY Zeuthen, 11.09.2018

IR/THz SASE source for pump-probe experiments @E-XFEL

PITZ-like accelerator can enable high power, tunable, synchronized IR/THz radiation

European XFEL (~3.4 km)

PITZ-like accelerator based
THz source (~20 m) →

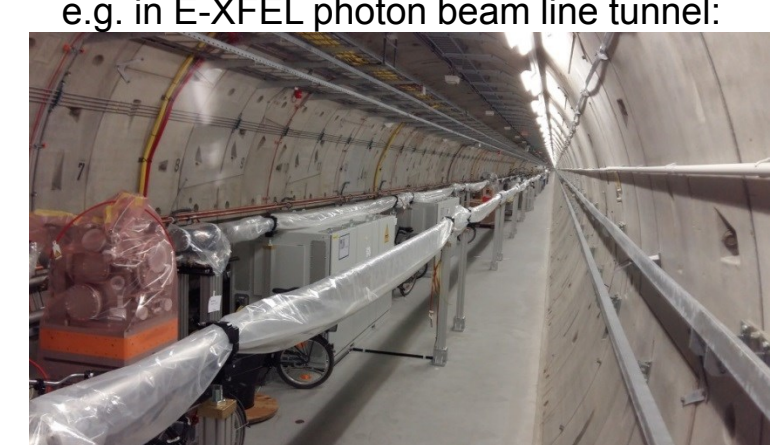
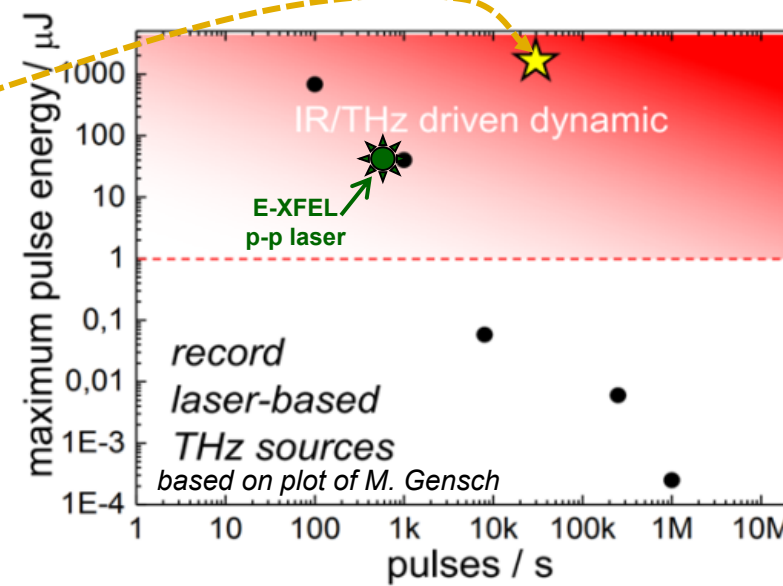
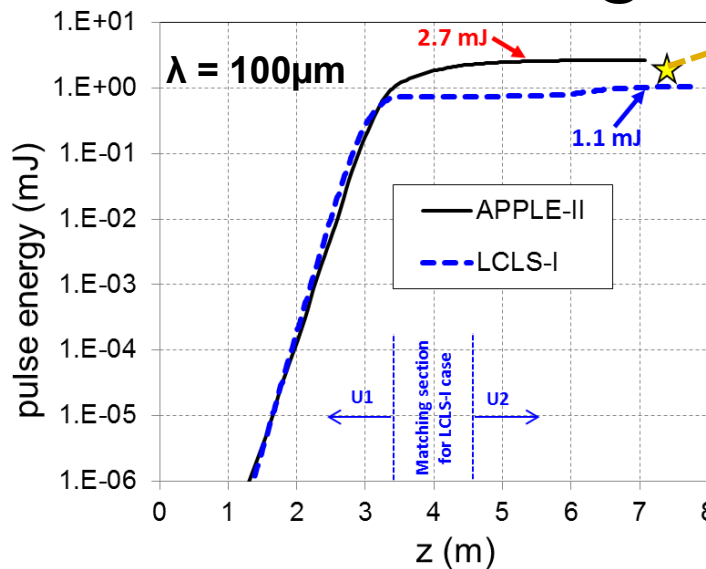


E.A. Schneidmiller, M.V. Yurkov, (DESY, Hamburg), M. Krasilnikov, F. Stephan, (DESY, Zeuthen),

"Tunable IR/THz source for pump probe experiments at the European XFEL, Contribution to FEL 2012, Nara, Japan, August 2012"

- Accelerator based IR/THz source **meets requirements** for pump-probe experiments (e.g. **the same pulse train structure !**)
- Construction of **radiation shielded area** for installing reduced copy of PITZ is possible close to user experiments at E-XFEL
- Prototype** of accelerator already exists → **PITZ** facility at DESY in Zeuthen

Simulation of THz SASE FEL @PITZ



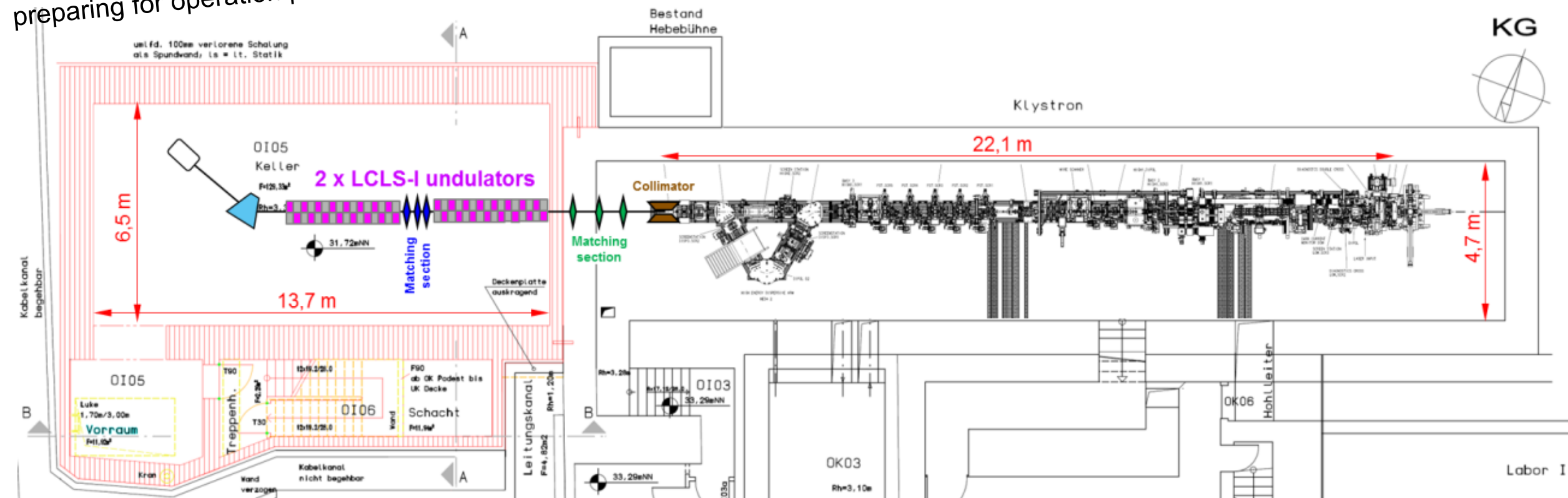
Required beam ($\sim 4\text{nC}$, $I_{\text{peak}} \sim 200\text{A}$)
already demonstrated at PITZ

→ **PITZ can be used for proof of principle and optimization!**

Planned installation of LCLS-I undulators in PITZ tunnel annex

Will be used for proof-of-principle experiments at PITZ

Currently improving radiation shielding and
preparing for operation permission for tunnel annex



SASE FEL based on PITZ accelerator and LCLS-I undulators

LCLS-I undulators (available on loan from SLAC) → under study and negotiations

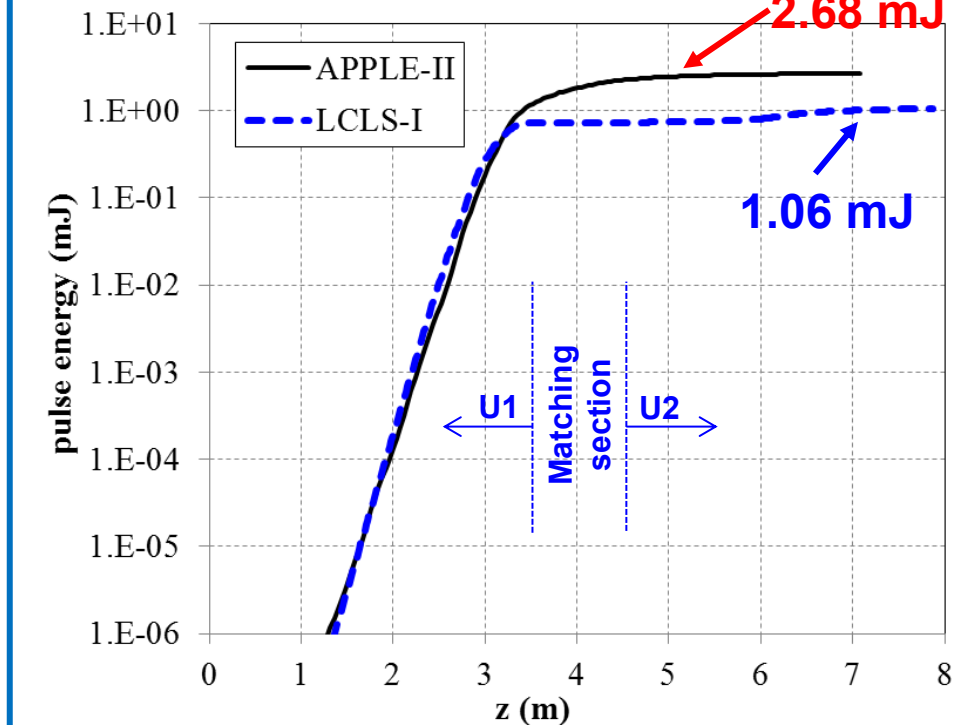
Some Properties of the LCLS-I undulator

Properties	Details
Type	planar hybrid (NdFeB)
K-value	3.49
Support diameter / length	30 cm / 3.4 m
Vacuum chamber size	11 mm x 5 mm
Period length	30 mm
Periods / a module	113 periods

Reference: LCLS conceptual design report, SLAC-0593, 2002.



Preliminary GENESIS Simulations ($\lambda_{rad}=100\mu\text{m}$)



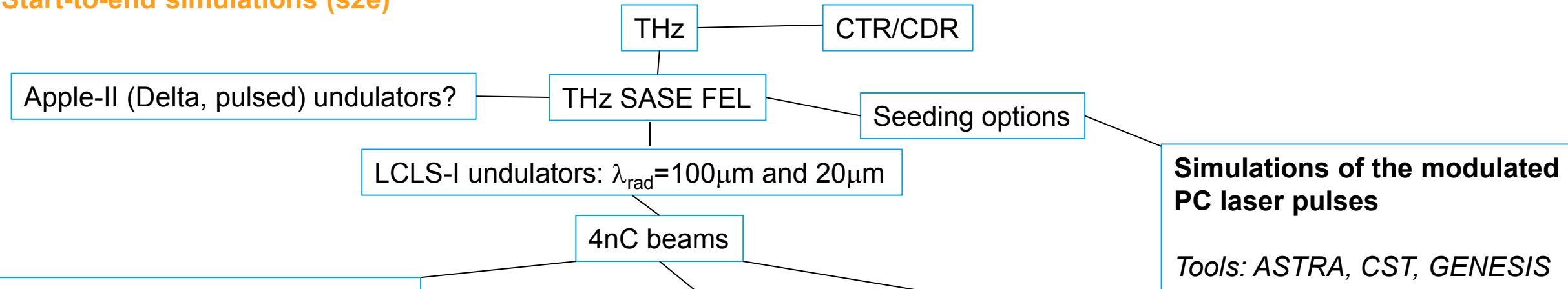
Preliminary conclusions on LCLS-I undulators at PITZ:

- Not such extremely high performance as for the APPLE-II, but is clearly proper for the proof-of-principle experiment!
- 4 nC electron beam transport through the vacuum chamber needs efforts, but seems to be feasible.

$$\lambda_{rad}=100\mu\text{m} \rightarrow \langle Pz \rangle = 16.65\text{MeV}/c$$

PITHz: THz proof-of-principle experiments at PITZ

Start-to-end simulations (s2e)



Generation

and transport to EMSY1

- 21.5ps FT PC laser
- Ø5mm (6.4mm opti)
- Optimized emittance at EMSY1
- Booster amplitude and phase → final P_z and min δE @ undulator

Open??:

- Realistic laser Ø, C+H
- Other temporal profiles
- Optimized emittance downstream EMSY1

Tools: ASTRA

Transport → undulators

Using:

- Existing quads
- Implementing new quads (realistic positioning in the PITZ beamline)

Open??:

- Beamline layout upgrade (quads, steerers, diagnostics)
- Precise position of U1 (after the wall)
- Collimator section

Tools: SC-soft, ASTRA, ...

Transport through undulators and THz generation

Narrow chamber effects

- Space charge
- Wakefields
- Waveguide effects

Open??:

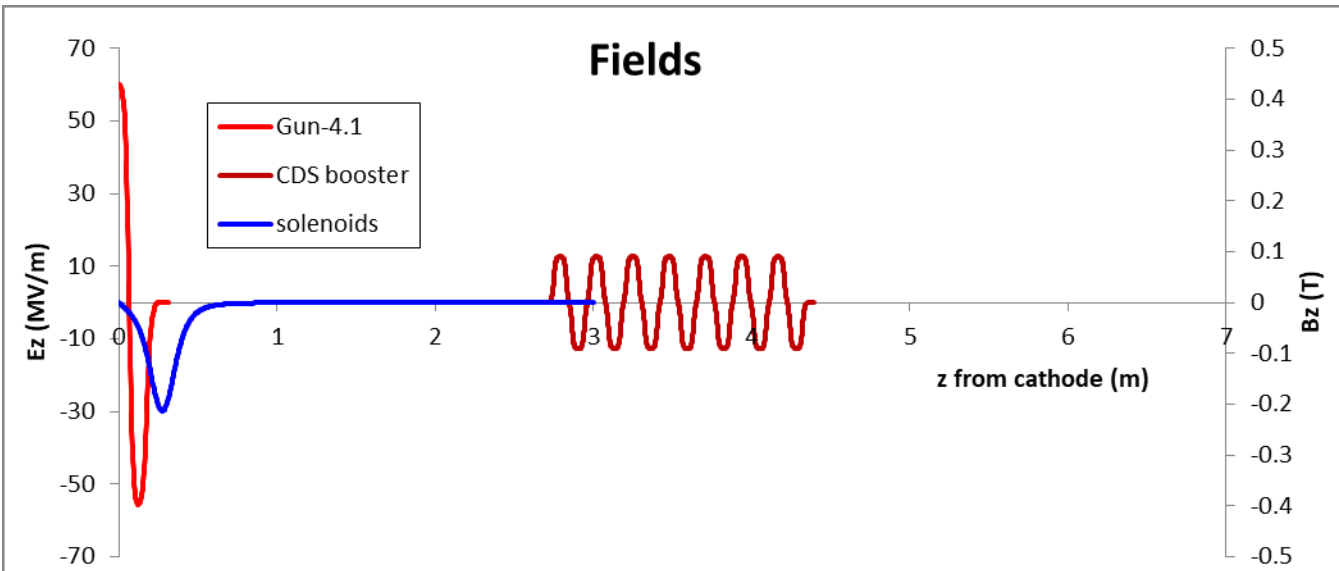
- Position of U2, matching section

Tools: SC-soft, ASTRA, CST, GENESIS, ...

Beam Dynamics Simulation Setup

ASTRA, SC-optimizer

Gun +Solenoids + CDS-booster



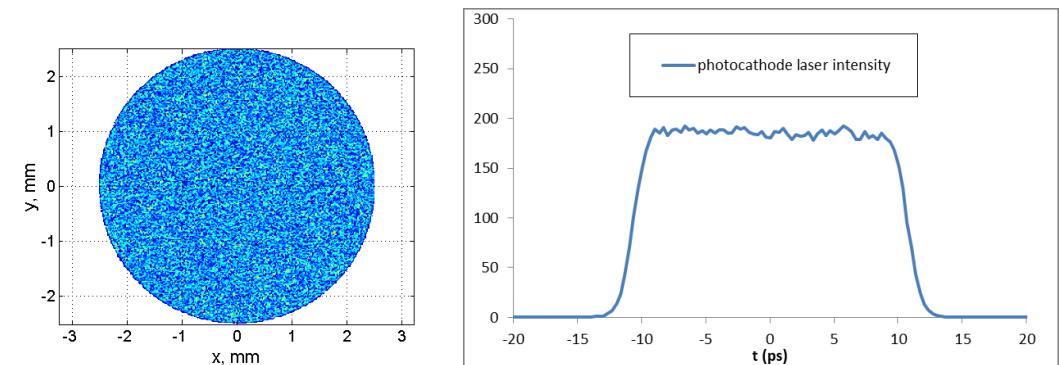
Gun:

- Ecath=60MV/m (fixed)
- MMMG

Booster:

- Emax<20MV/m
 - Phase=phi2*
- } $\rightarrow \langle P_z \rangle = 16.7 \text{ MeV}/c + \min \delta E @ \text{undulator?}$

Photocathode laser



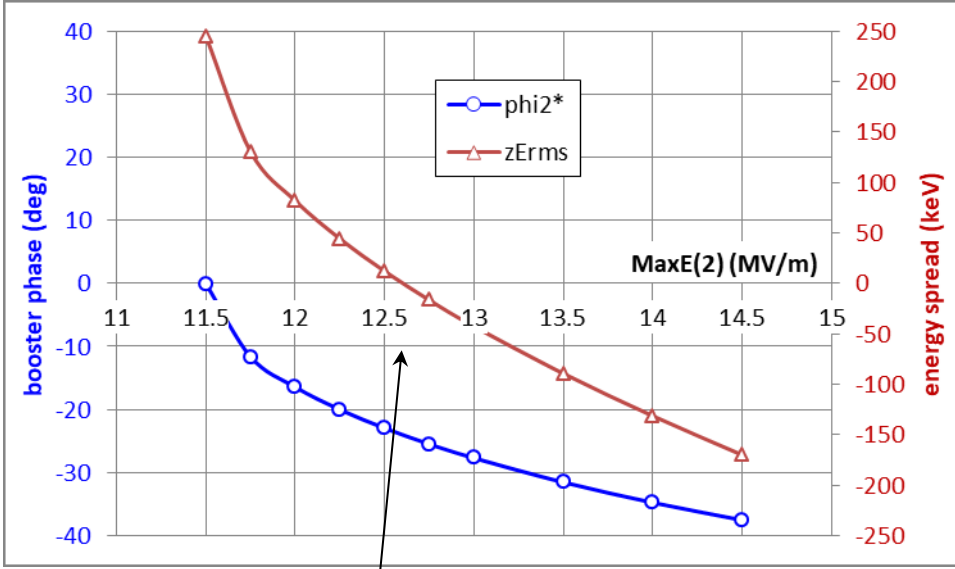
Photocathode laser:

- FT 21.5ps FWHM
- $\emptyset \leq 5\text{mm}$
- 4nC

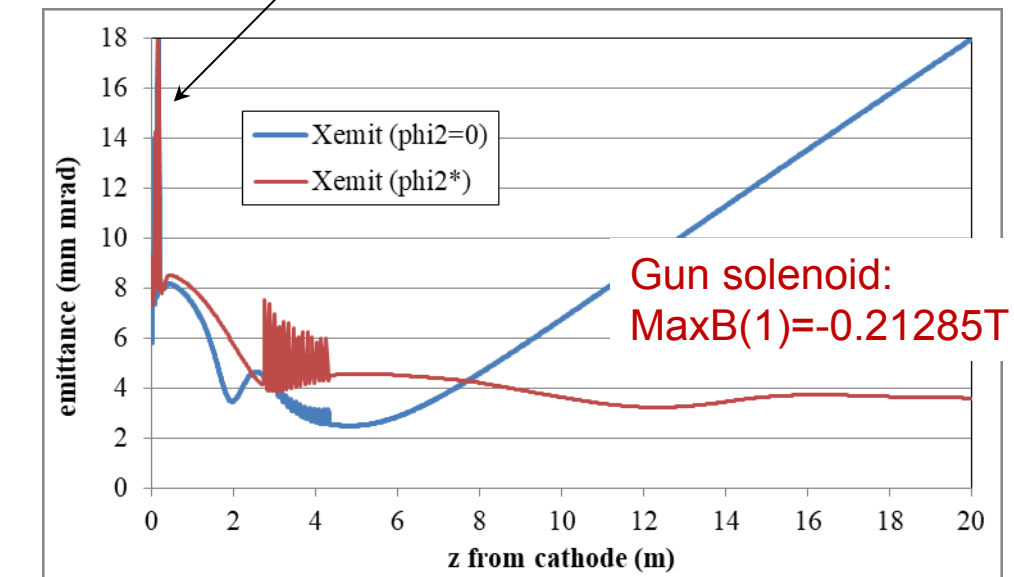
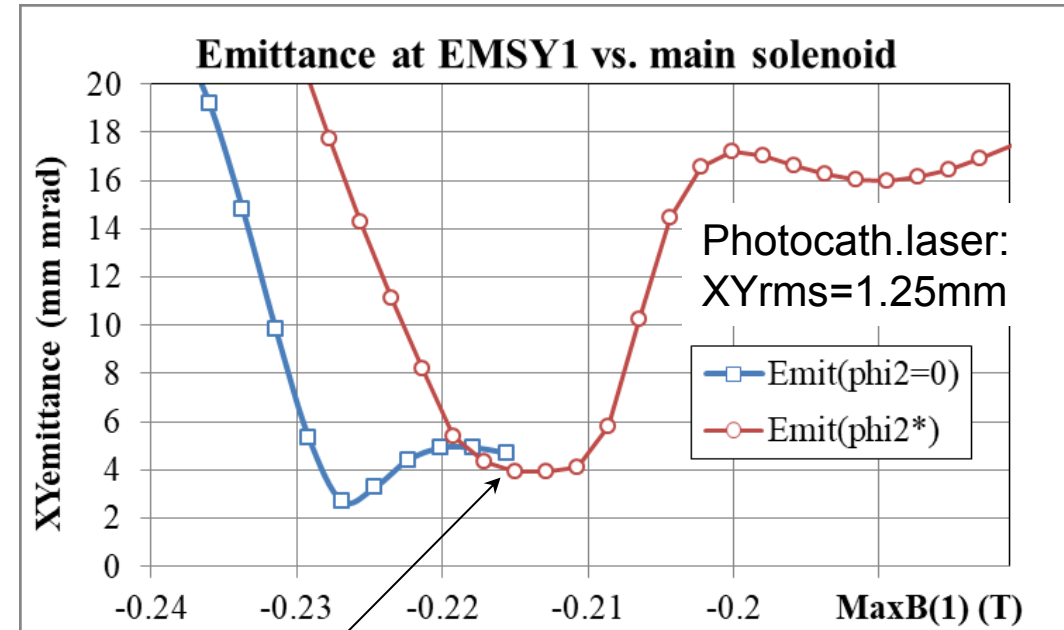
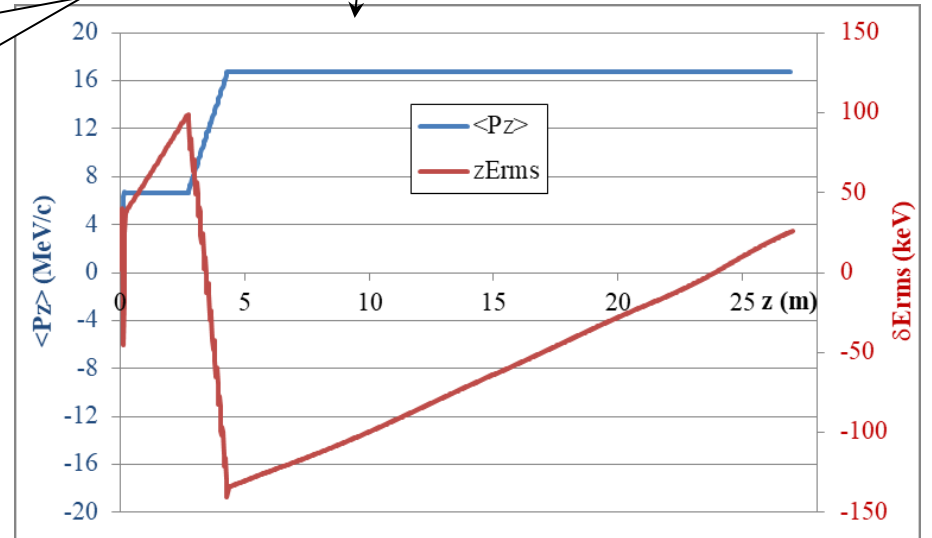
Gun, solenoid, booster parameters

Extremely small emittance is not a goal

ϕ_{2^*} = booster phase for
 $\langle P_z \rangle = 16.7 \text{ MeV}/c$

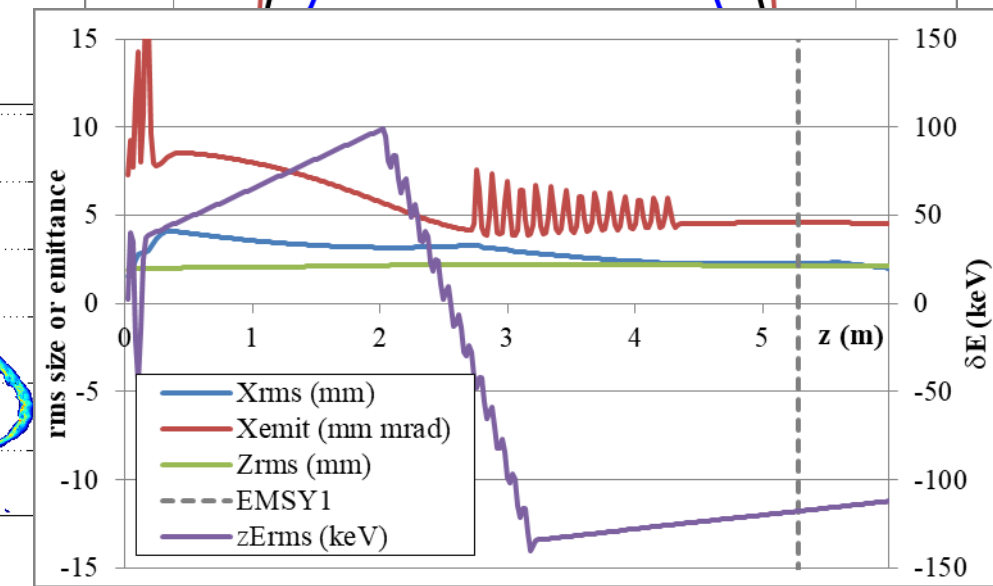
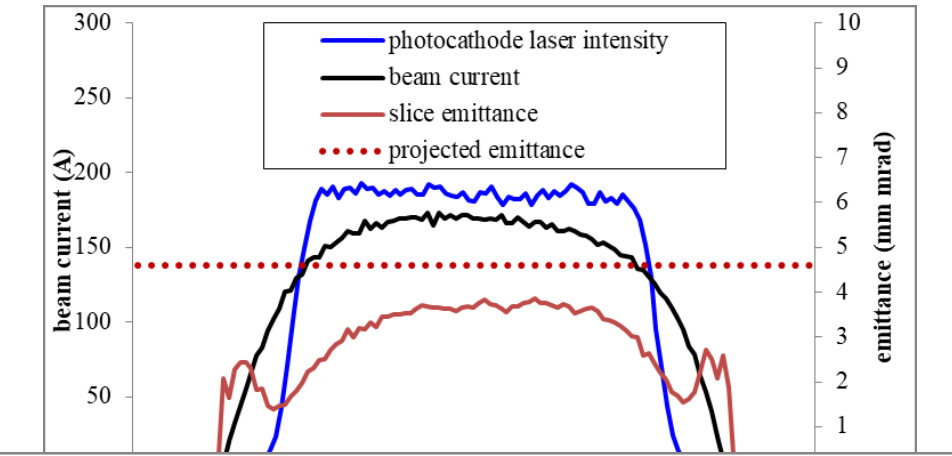
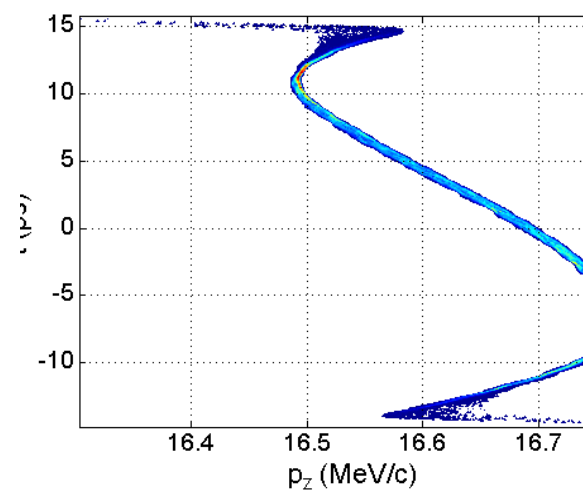
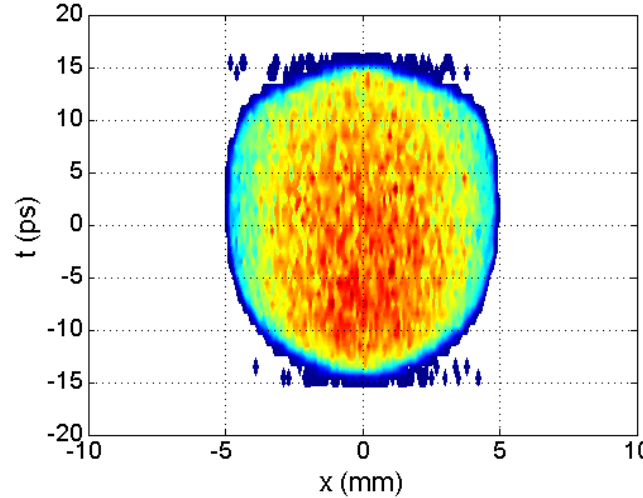
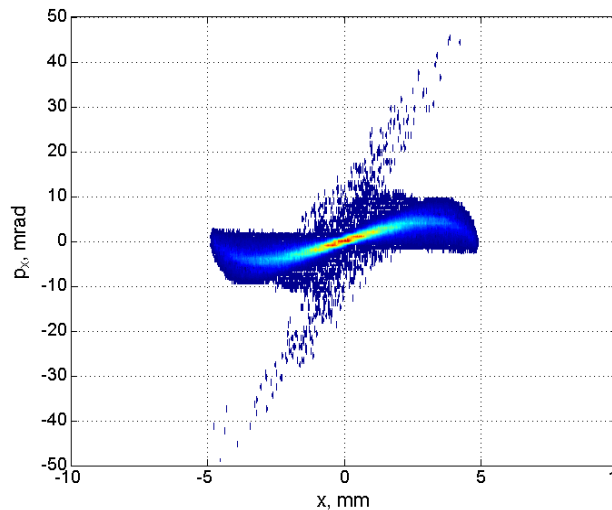
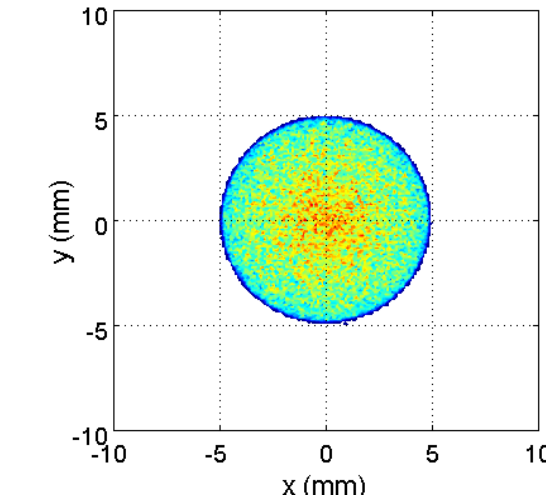


Booster:
 $\text{MaxE}(2) = 12.6 \text{ MV/m}$
 $\Phi(2) = -24 \text{ deg}$



Beam at EMSY1 – “ready” for transport

Z=5.277m from the cathode



Estimations on beam size in a drift

Based on method of moments w/o space charge

Second order moment of beam distribution function:

$$M_{\mu\nu} = \langle (\mu - \langle \mu \rangle)(\nu - \langle \nu \rangle) \rangle, \text{ where } \mu, \nu = x, y, p_x, p_y.$$

A simple model results in a system of ODE for e.g. x-plane:

$$\frac{dM_{p_x p_x}}{d\tau} = 2\kappa \frac{M_{x p_x}}{M_{x x}}, \quad \frac{dM_{x p_x}}{d\tau} = \frac{M_{p_x p_x}}{\gamma}, \quad \frac{dM_{x x}}{d\tau} = \frac{2}{\gamma} M_{x p_x}$$

κ is a space charge related factor (let us assume $\kappa = 0$ for the first approximation), $\tau = ct$. Assuming start from the beam waist ($M_{x p_x}(0) = 0$; $M_{x x}(0) = \sigma_0^2$), the solution of the ODE can be represented as:

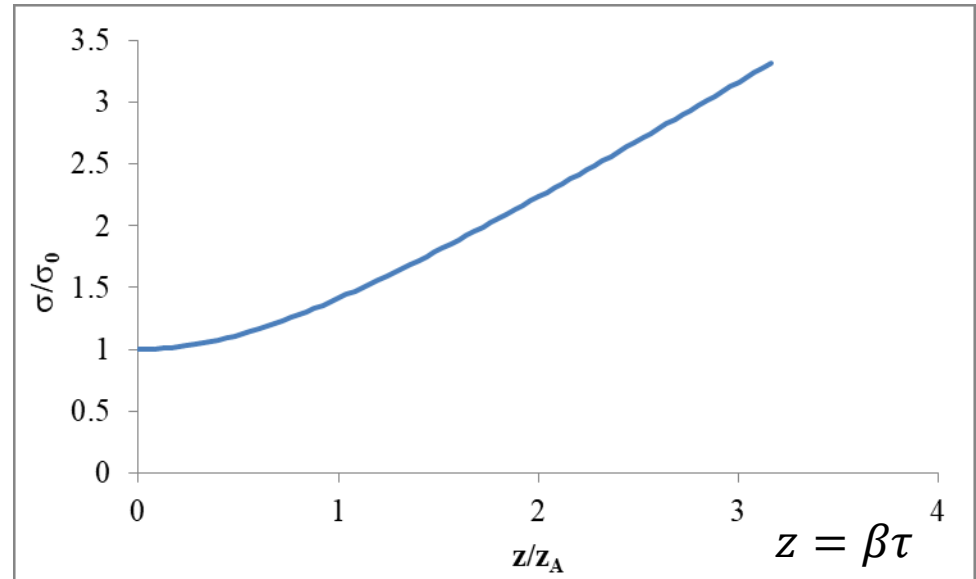
$$M_{p_x p_x}(\tau) = M_{p_x p_x}(0)$$

$$M_{x p_x}(\tau) = \frac{M_{p_x p_x}(0)}{\gamma} \tau$$

$$M_{x x}(\tau) = \sigma_0^2 + \frac{M_{p_x p_x}(0)}{2\gamma} \tau^2$$

Beam emittance is invariant for these conditions:

$$\varepsilon_{n,x}^2 = M_{x x} M_{p_x p_x}(0) - M_{x p_x}^2 = \sigma_0^2 M_{p_x p_x}^2(0) = \text{const}$$



$$M_{x x}(z) = \sigma_0^2 + \frac{\varepsilon_{n,x}^2}{2\gamma\beta^2\sigma_0^2} z^2$$

Denoting $z_A = \frac{\sigma_0^2\beta}{\varepsilon_{n,x}} \sqrt{2\gamma}$, one obtains

$$\frac{\sigma}{\sigma_0} = \frac{\sqrt{M_{x x}(z)}}{\sigma_0} = \sqrt{1 + \frac{z^2}{z_A^2}}$$

Estimations on beam size in a drift

Based on method of moments w/o space charge

$$M_{xx}(z) = \sigma_0^2 + \frac{\varepsilon_{n,x}^2}{2\gamma\beta^2\sigma_0^2} z^2$$

$$\sigma^2(z = L, \sigma_0) = \sigma_0^2 + \frac{\varepsilon_{n,x}^2}{2\gamma\beta^2\sigma_0^2} L^2$$

$L = \frac{L_U}{2}$ is a half undulator length,

$$\frac{\partial \sigma}{\partial \sigma_0} = 0 \rightarrow \sigma_{0,min} = \sqrt{\frac{\varepsilon_{n,x} L}{\beta \sqrt{2\gamma}}}$$

$$\sigma(z = L, \sigma_{0,min}) = \sqrt{2}\sigma_{0,min} = \sqrt{\sqrt{\frac{2\varepsilon_{n,x} L}{\gamma \beta}}}$$

Applying obtained beam parameters:

$$\varepsilon_{n,x} = 4 \cdot 10^{-6} m \text{ rad}$$

$$L = \frac{L_U}{2} = 1.7 \text{ m}$$

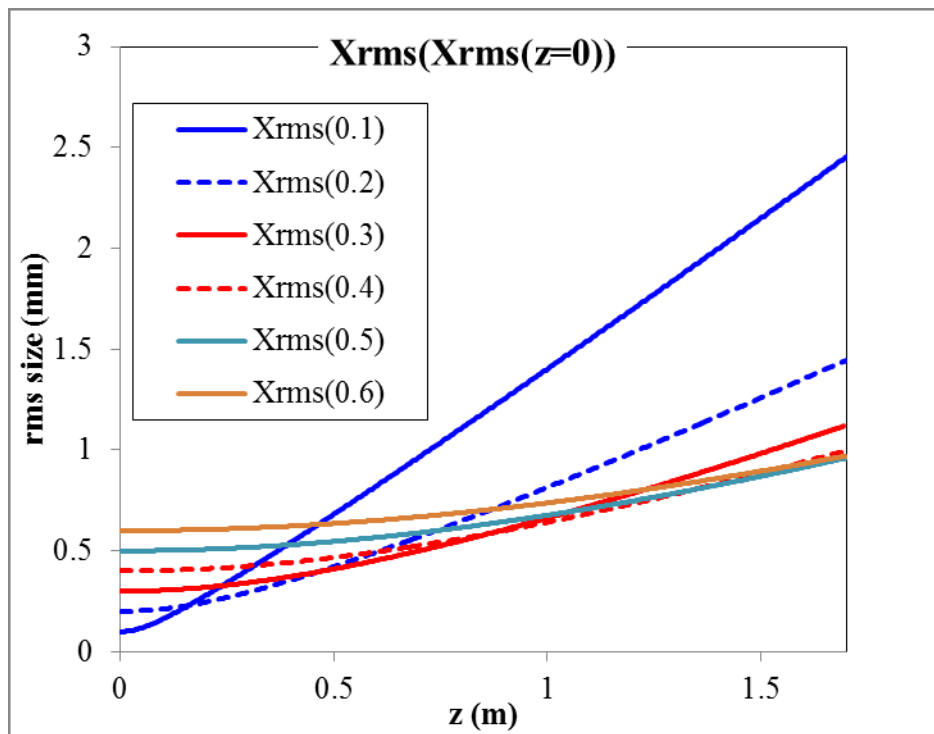
$$\gamma = 32.6$$

$$\beta = 0.9995$$

$$\sigma(z = L, \sigma_{0,min}) \approx \mathbf{1.3 \text{ mm}}$$

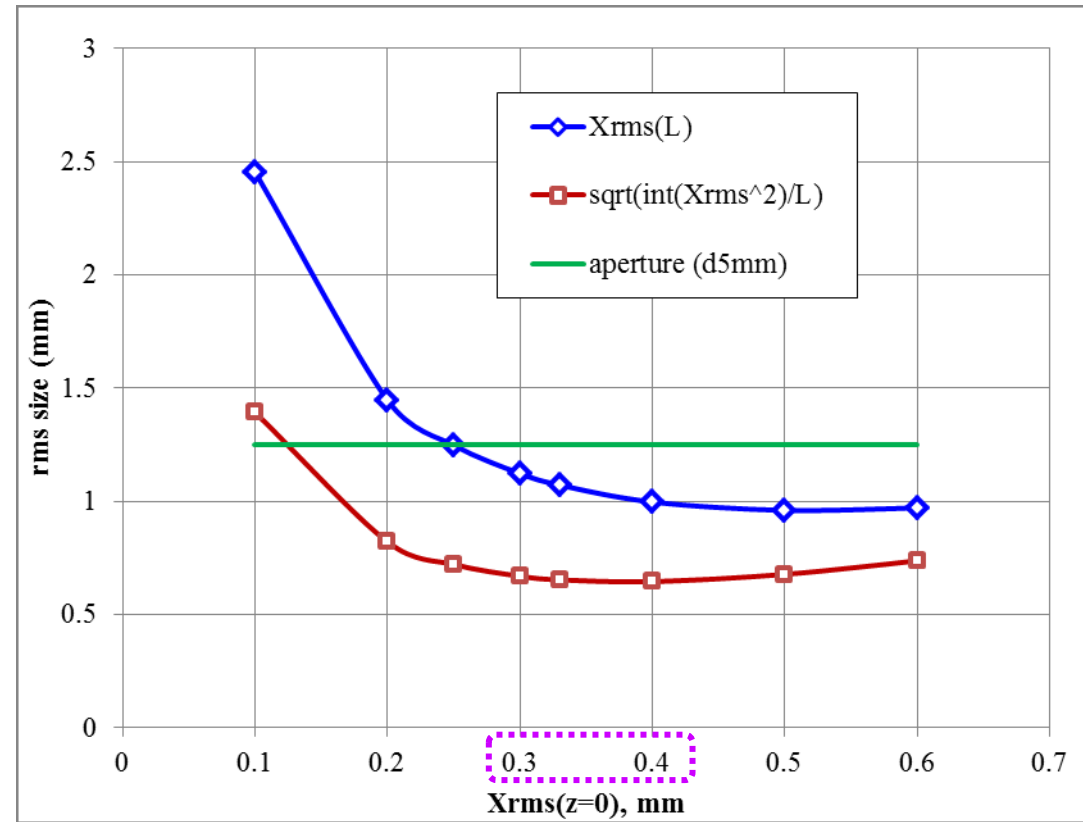
Estimations on beam size in a drift

Based on ASTRA simulations with space charge



"Ideal" electron beam:

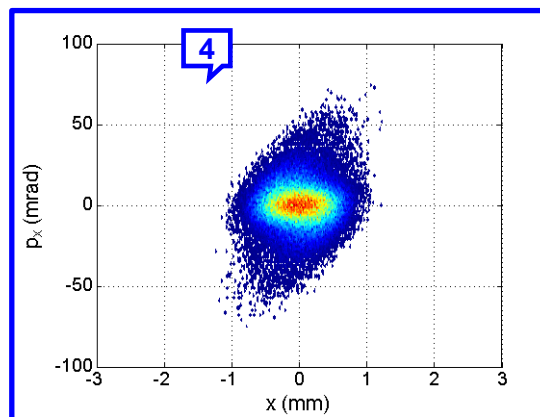
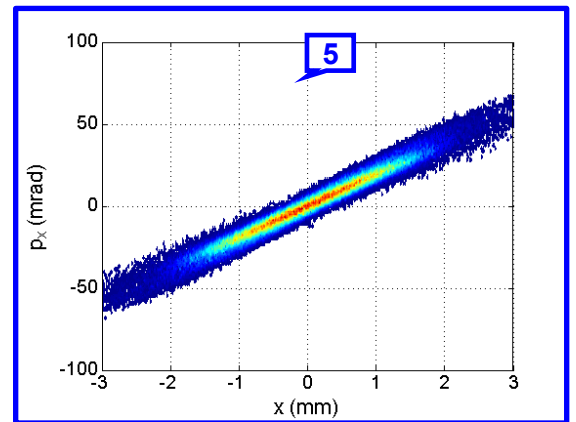
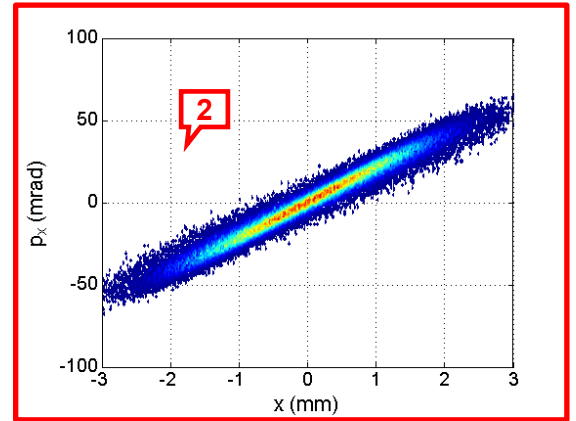
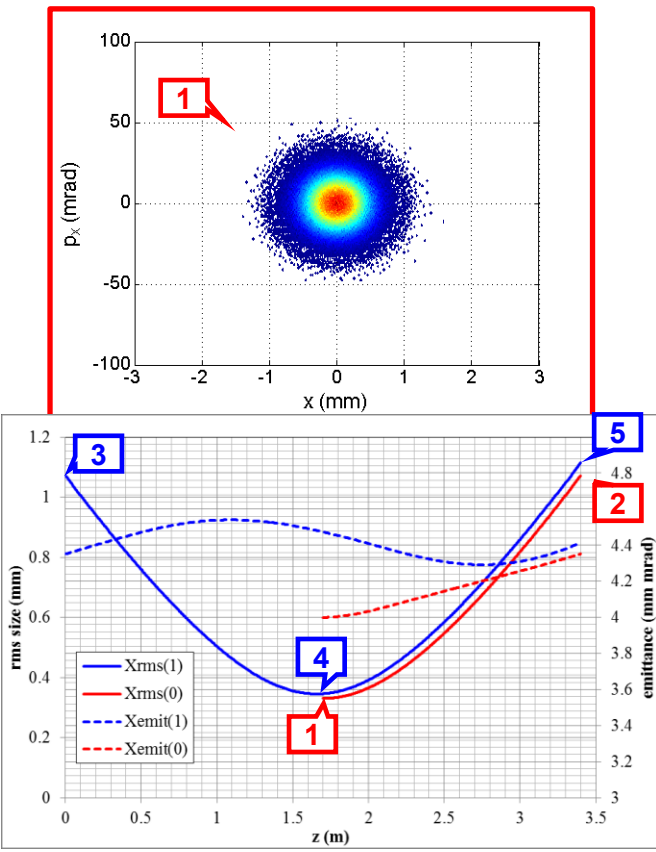
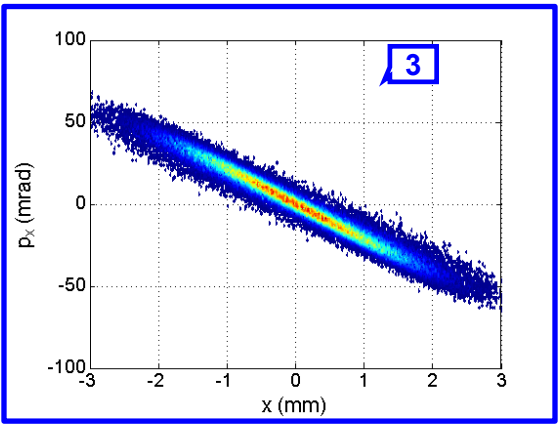
- Q=4nC
- Temporal: FT, 7ps FWHM
- Transverse phase space: Gaussian
- <P_z>=16.7MeV/c
- ε(z=0)=4 mm mrad



$$GF(X_{rms,0}) = \sqrt{\frac{1}{L} \int_0^L X_{rms}^2 dz}$$

Estimations on beam size in a drift

Based on ASTRA simulations with space charge



“Ideal” (Gaussian-FT) electron beam:

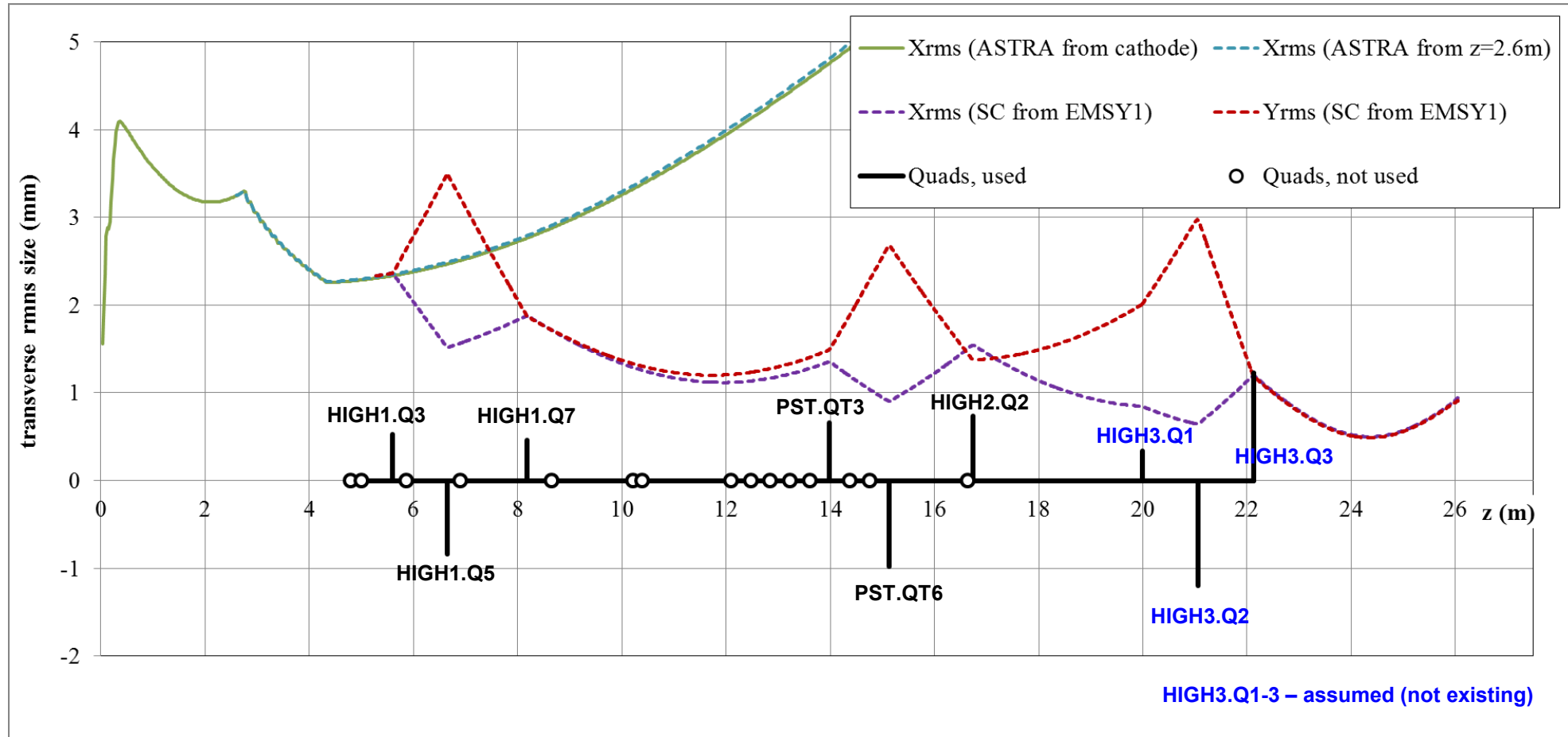
- $Q=4nC$
- $\langle P_z \rangle = 16.7 \text{ MeV}/c$
- $\varepsilon \sim 4 \text{ mm mrad}$

can be transported through pipe:

- $L=3.4\text{m}$
- $\emptyset 5\text{mm}$

PITZ Beam from the cathode → tunnel wall

ASTRA→ SC-optimizer



NB: ASTRA Space Charge 3D:

200k particles $\rightarrow N_{x,y,z}=16 \rightarrow 13$ part/cell

200k particles $\rightarrow N_{x,y,z}=32 \rightarrow 191$ part/cell

$$GF(Q_1, \dots, Q_9) \propto \sqrt{\frac{1}{L} \int_0^L X_{\text{rms}} \cdot Y_{\text{rms}} dz}$$

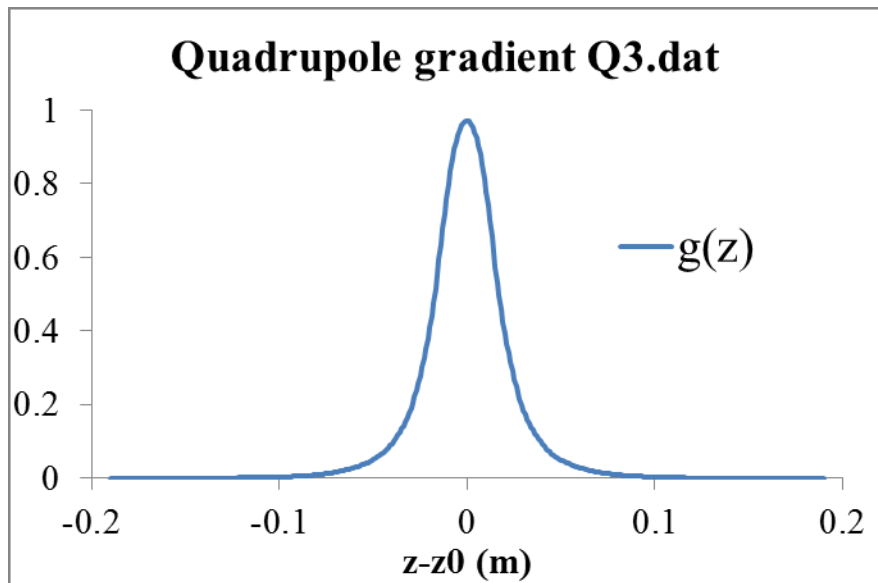
SC → ASTRA

Quadrupole “recalibration”

- SC-optimizer → Hard edge model

A. Matvienko “Effective length of the thick lens”: $L_{eff} = \frac{6 \int_{-\infty}^{\infty} \left[\int_{-\infty}^z g(z_1) dz_1 \cdot \int_z^{\infty} g(z_2) dz_2 \right] dz}{\left[\int_{-\infty}^{\infty} g(z) dz \right]^2}$

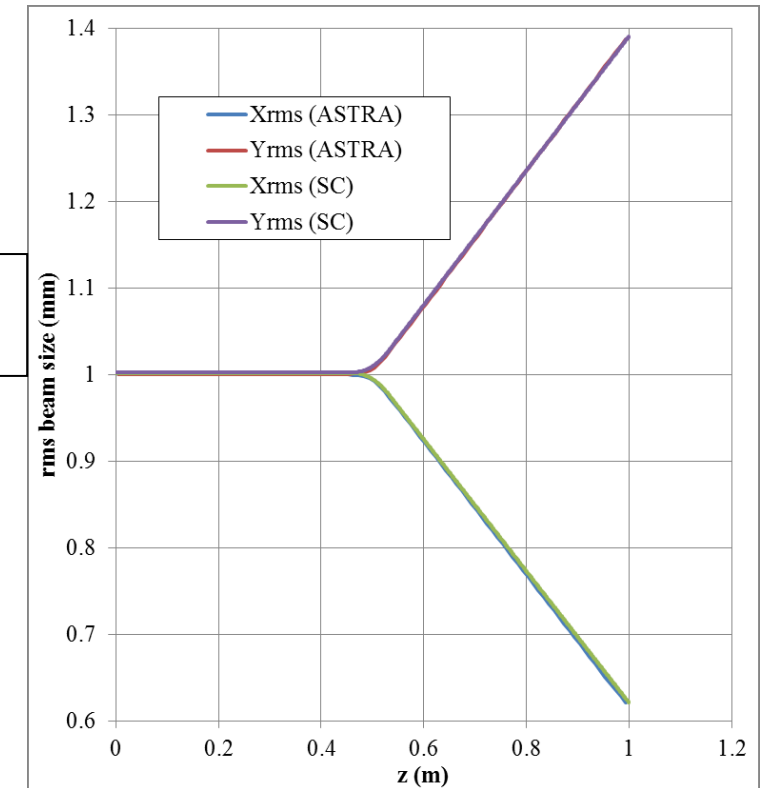
- ASTRA → Measured gradient Q3.dat



$$L_{eff} = 0.0675\text{m}$$

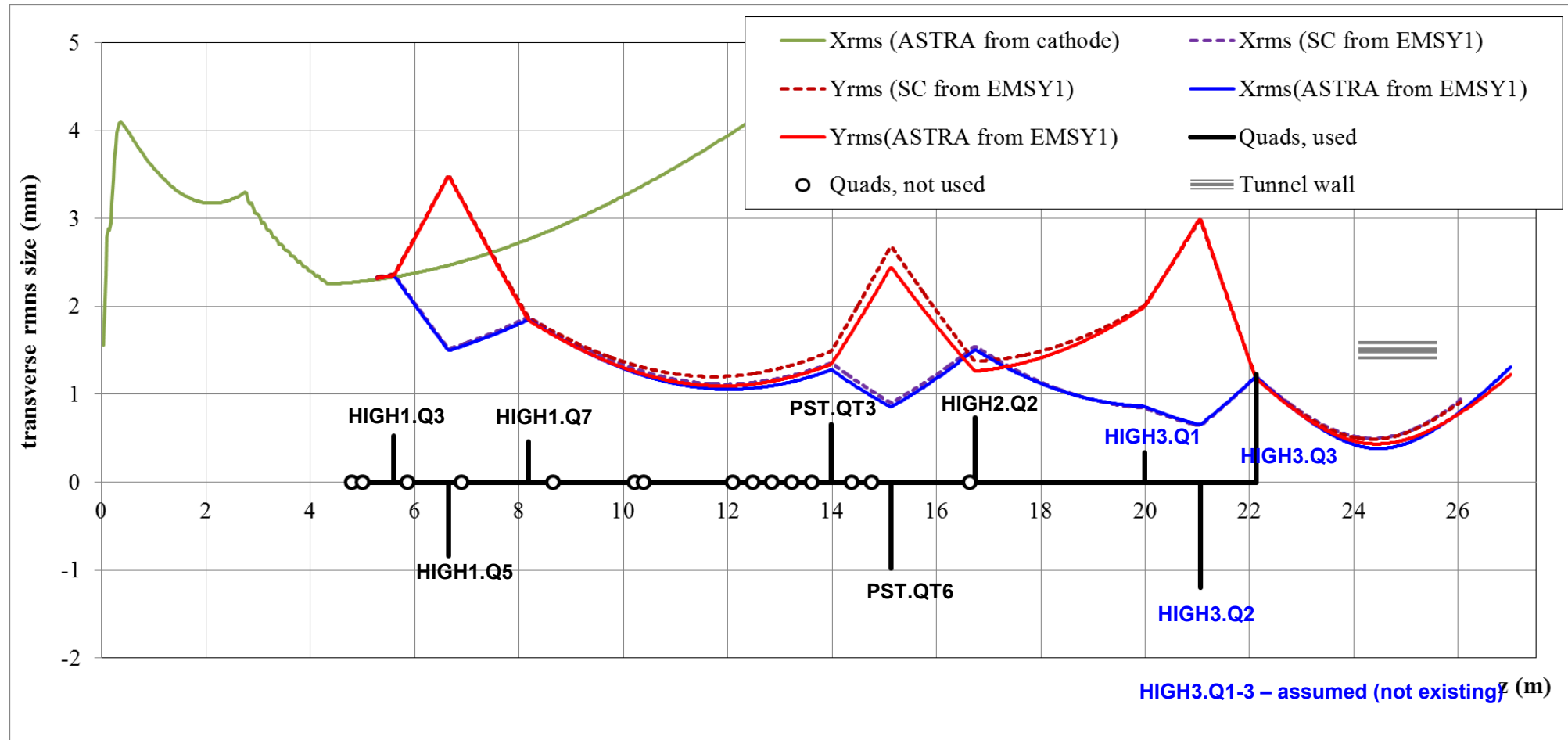
Cross-check:
SC ↔ ASTRA

ASTRA	SC-optimizer
Q3.dat Q_grad=1T/m	Length=0.0675 Gradient=0.625T/m



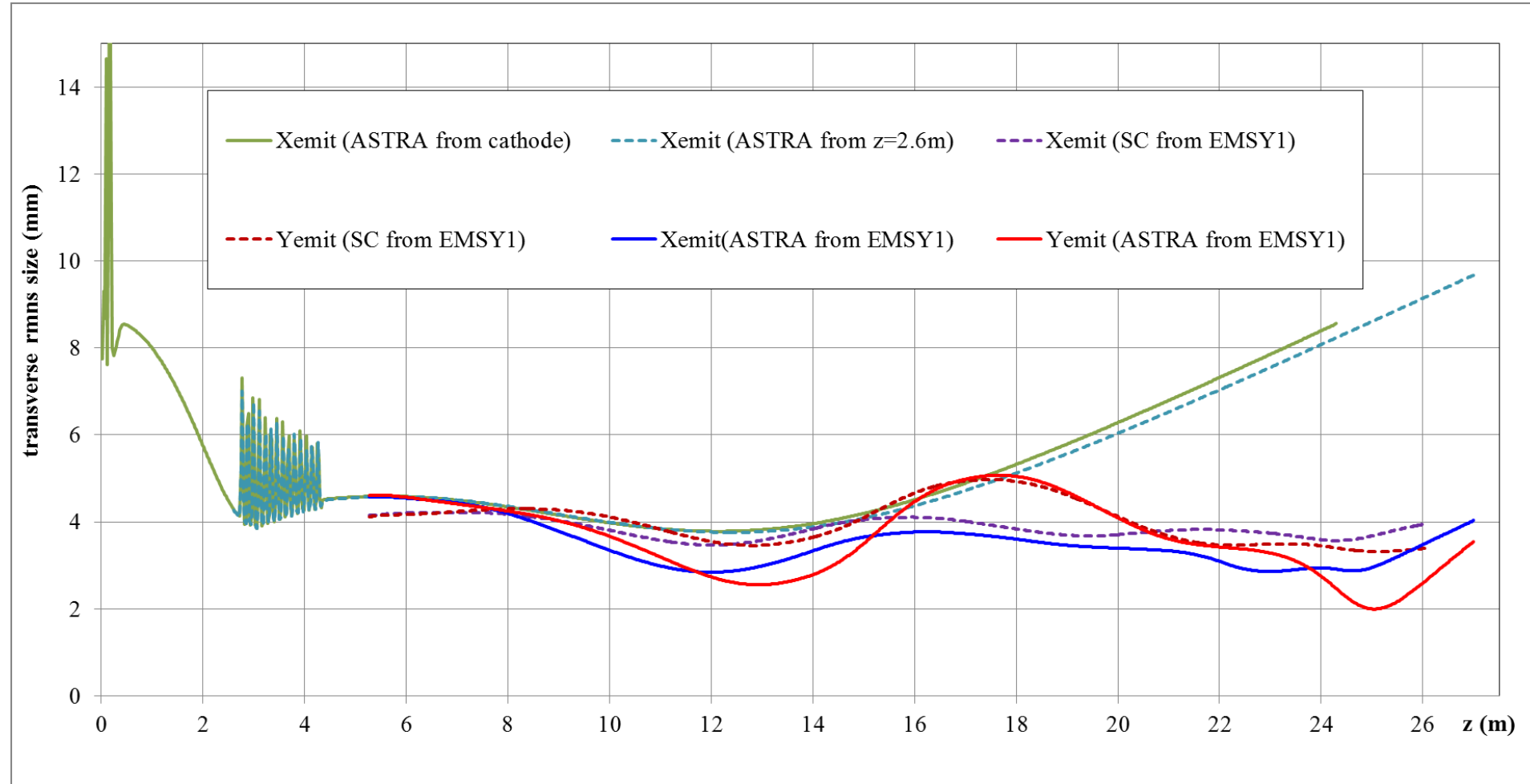
PITZ Beam from the cathode → tunnel wall

ASTRA check



PITZ Beam from the cathode → tunnel wall

Beam emittance using SC-optimizer and ASTRA

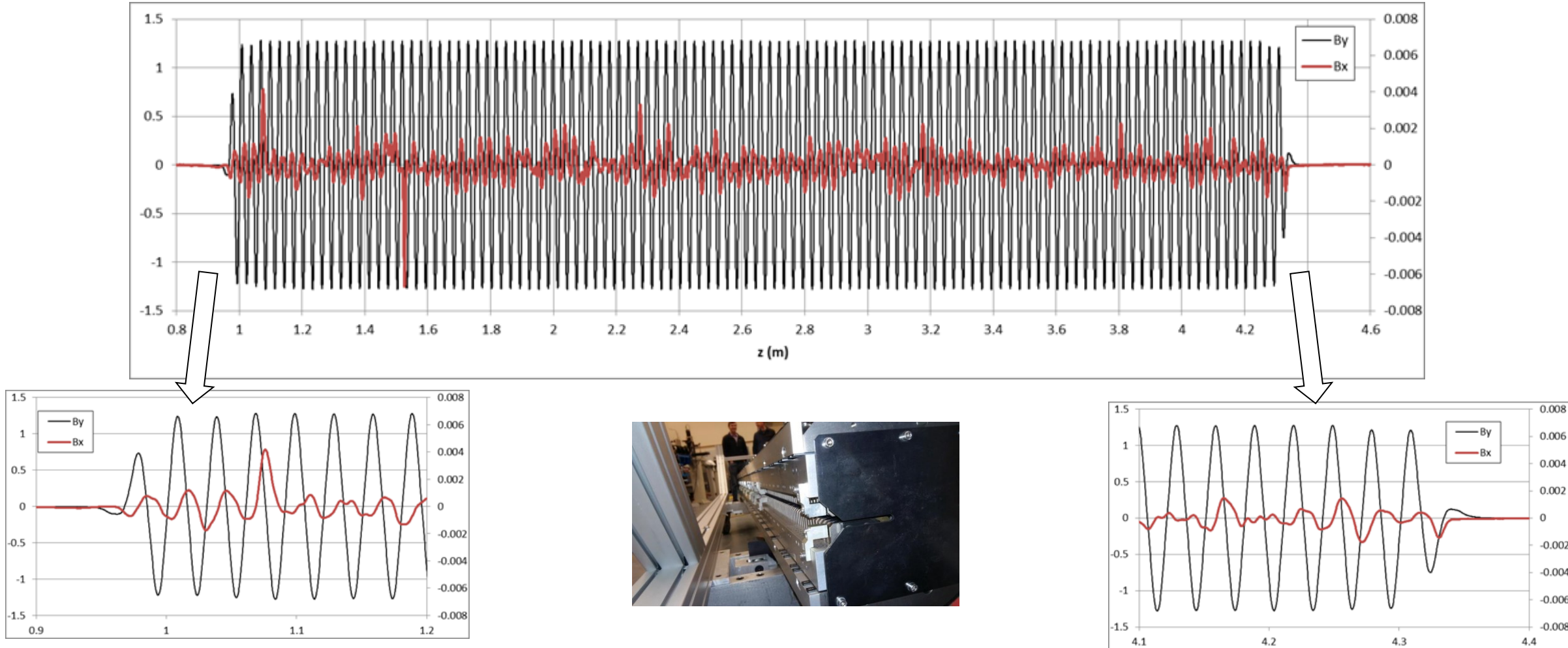


S2E simulations: 4nC 16.7MeV/c beam transport from the cathode till and through the tunnel wall → OK

LCLS-I Undulator field

By(z) field profile measurements done on 02.10.2013 at SLAC for the undulator L143-112000-07 after the final tuning

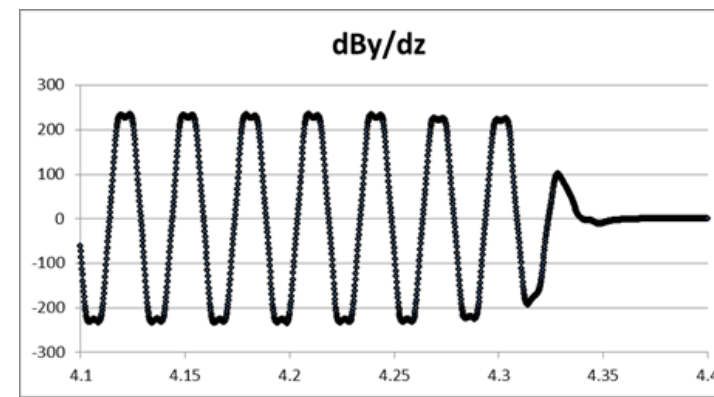
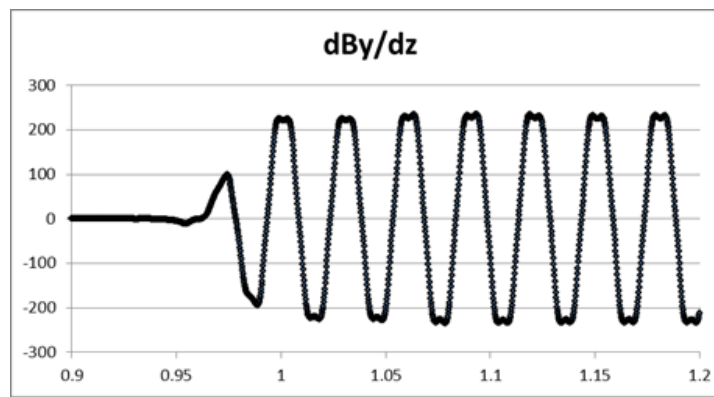
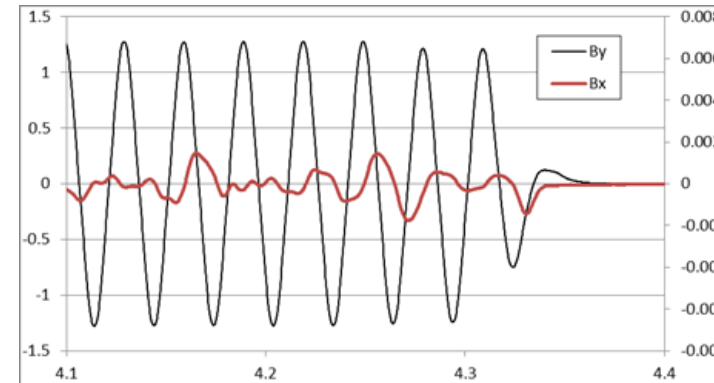
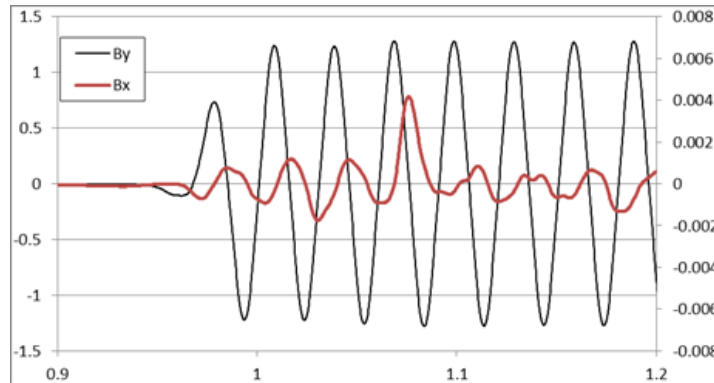
Based on file x+00000_y+000_bscanz.dat (communication with Heinz-Dieter Nuhn from 06.07.2018)



LCLS-I Undulator field

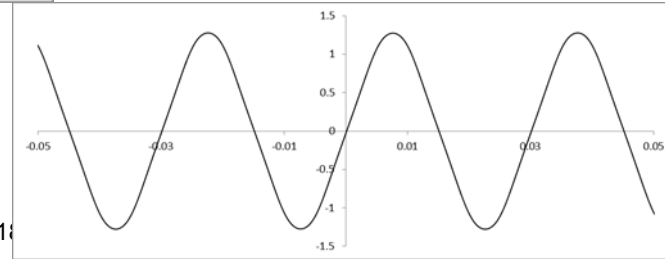
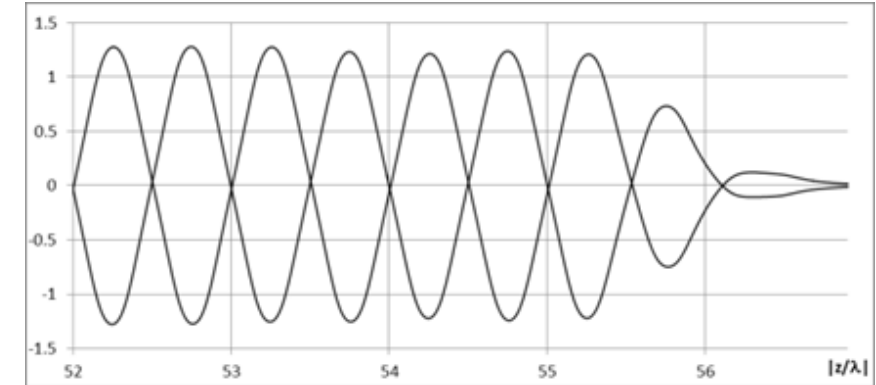
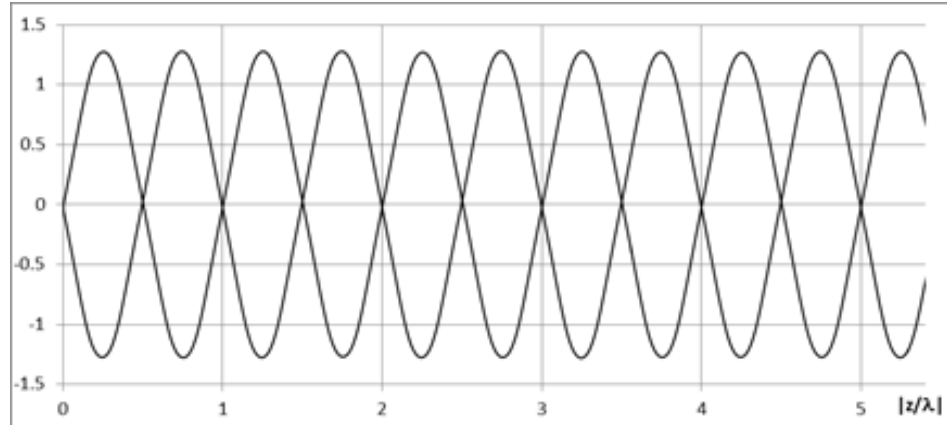
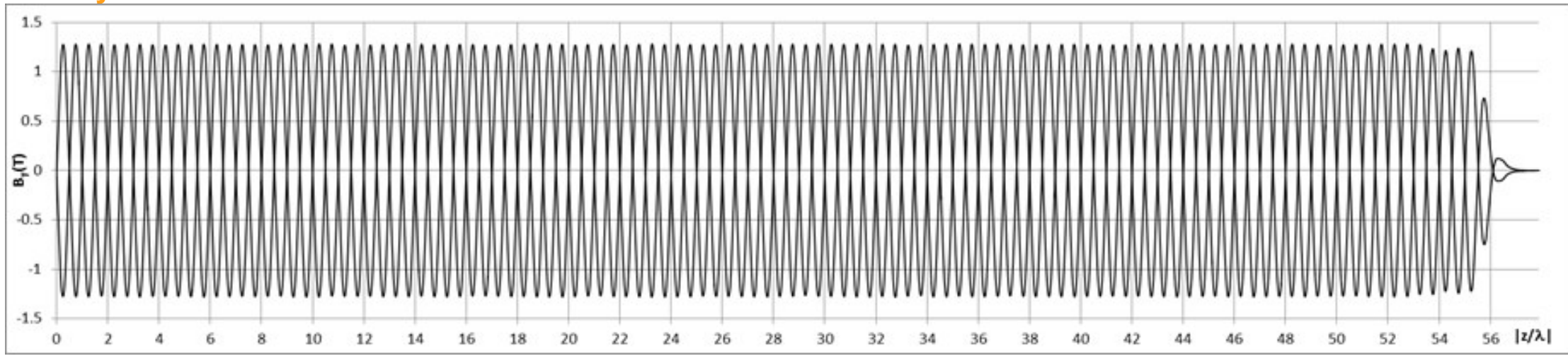
By(z) field profile measurements done on 02.10.2013 at SLAC for the undulator L143-112000-07 after the final tuning

Based on file `x+00000_y+000_bscanz.dat` (communication with Heinz-Dieter Nuhn from 06.07.2018)



LCLS-I Undulator field

Fourier Analysis



LCLS-I Undulator field

Fourier Analysis

Performing Fourier transformation for $-\frac{L}{2} \leq z \leq \frac{L}{2}$, where $L = N_U \lambda_U$ is the undulator length:

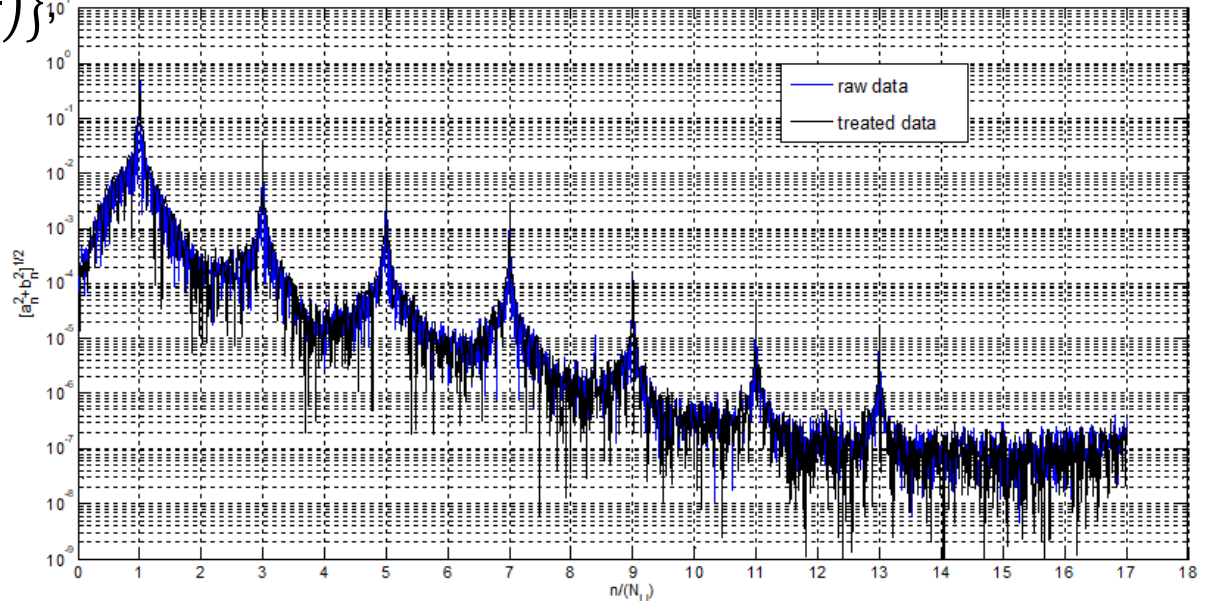
$$B_y(x = 0, y = 0, z) = \sum_{n=0}^{\infty} \left\{ a_n \cos \left(\frac{2\pi n z}{N_U \lambda_U} \right) + b_n \sin \left(\frac{2\pi n z}{N_U \lambda_U} \right) \right\}$$

where

$$a_n = \frac{2}{L} \int_{-\frac{L}{2}}^{\frac{L}{2}} B_y(x = 0, y = 0, z) \cos \left(\frac{2\pi n z}{N_U \lambda_U} \right) dz,$$

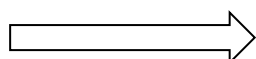
$$a_0 = \frac{1}{L} \int_{-\frac{L}{2}}^{\frac{L}{2}} B_y(x = 0, y = 0, z) dz,$$

$$b_n = \frac{2}{L} \int_{-\frac{L}{2}}^{\frac{L}{2}} B_y(x = 0, y = 0, z) \sin \left(\frac{2\pi n z}{N_U \lambda_U} \right) dz.$$

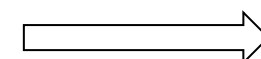


Field integrals of the undulator:

$$I_{1y} = \int_{-\frac{L}{2}}^{\frac{L}{2}} B_y(x = 0, y = 0, z) dz,$$

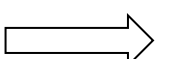


$$I_{1y} = a_0 L,$$

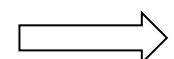


$$a_0 = 0$$

$$I_{2y} = \int_{-\frac{L}{2}}^{\frac{L}{2}} dz \int_{-\frac{L}{2}}^z B_y(x = 0, y = 0, z_1) dz_1.$$



$$I_{2y} = \frac{L^2}{2} \left\{ a_0 + \sum_{n=1}^{\infty} \frac{(-1)^n}{\pi n} b_n \right\}$$



$$\sum_{n=1}^{\infty} \frac{(-1)^n}{\pi n} b_n = 0$$

LCLS-I Undulator field

“Improving “ the field profile

The procedure to generate **infinitely smooth $B_y(0,0,z)$** distribution antisymmetric w.r.t. $z=0$ includes several steps:

- Rough **centering** of the distribution $B_{y,raw}(z)$, so $B_{y,raw}(-z) \approx -B_{y,raw}(z)$,
- Determination of $N_U = L/\lambda_U$ the for **Fourier transformation** of the measured data,
- Determination of the **background** based on the left $B_{y,bkg-left} = B_{y,bkg}(-L/2)$ and right

$$B_{y,bkg-right} = B_{y,bkg}(L/2) \text{ using linear dependence: } B_{y,bkg}(z) = B_{y,bkg-left} + \frac{B_{y,bkg-right} - B_{y,bkg-left}}{L}.$$

- **Subtraction of the background**: $B_{y,1}(z) = B_{y,raw}(z) - B_{y,bkg}(z)$
- **Fine centering** of the obtained distribution $B_{y,1}(z_1 = z - z_0)$, so $B_{y,1}(z_1 = 0) = 0$,
- **Symmetrizing** the distribution $B_{y,2}(z_2) = \frac{B_{y,2}(z_2) - B_{y,2}(-z_2)}{2}$ on the mesh z_2 which includes $z_2 = 0$ explicitly.

All these steps were included in the optimization procedure with following **optimization parameters**:

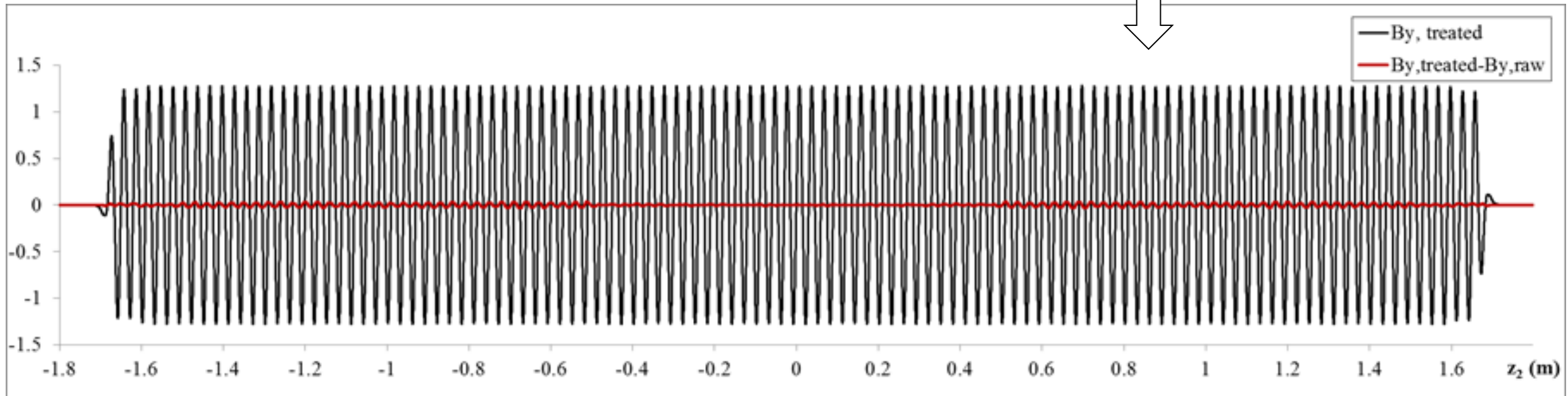
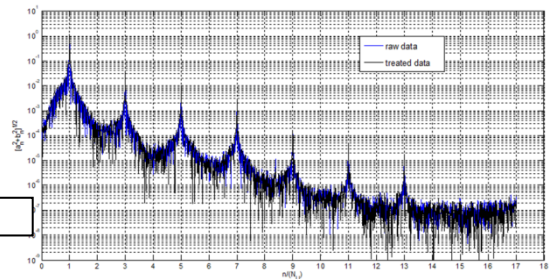
$$\{N_U, B_{y,bkg-left}, B_{y,bkg-right}\}, \text{ minimizing : } \Phi(N_U, B_{y,bkg-left}, B_{y,bkg-right}) = \sum_{n=1}^{N_h \cdot N_U} \frac{(-1)^n}{\pi n} \tilde{b}_n,$$

$$\text{where } \tilde{b}_n = \frac{2}{N_U \lambda_U} \int_{-\frac{N_U \lambda_U}{2}}^{\frac{N_U \lambda_U}{2}} B_{y,2}(x = 0, y = 0, z_1) \sin\left(\frac{2\pi n z_1}{N_U \lambda_U}\right) dz,$$

and the number of harmonics N_h is taken to be high enough ($N_h > 10$, typically, $N_h = 17$).

LCLS-I Undulator field

“Improving “ the field profile



$$B_{y,2}(0,0,z) = \sum_{n=1}^{N_h \cdot N_U} \left\{ \tilde{a}_n \cos\left(\frac{2\pi n z}{N_U \lambda_U}\right) + \tilde{b}_n \sin\left(\frac{2\pi n z}{N_U \lambda_U}\right) \right\}$$

LCLS-I Undulator field

3D field map generation

Scalar magnetic potential $\Psi(y, z)$ for the case of the field which is symmetric in the horizontal plane and homogeneous in horizontal:

$$\Psi(y, z) = \sum_{m=0}^{\infty} (-1)^m \frac{d^{2m} B_{y,2}(0,0,z)}{dz^{2m}} \cdot \frac{y^{2m+1}}{(2m+1)!}.$$

Applying differentiation to

$$B_{y,2}(0,0,z) = \sum_{n=1}^{N_h \cdot N_U} \left\{ \tilde{a}_n \cos \left(\frac{2\pi n z}{N_U \lambda_U} \right) + \tilde{b}_n \sin \left(\frac{2\pi n z}{N_U \lambda_U} \right) \right\}$$

$$\frac{d^{2m} B_{y,2}(0,0,z)}{dz^{2m}} = \sum_{n=1}^{N_h \cdot N_U} (-1)^m \left(\frac{2\pi n}{N_U \lambda_U} \right)^{2m} \left\{ \tilde{a}_n \cos \left(\frac{2\pi n z}{N_U \lambda_U} \right) + \tilde{b}_n \sin \left(\frac{2\pi n z}{N_U \lambda_U} \right) \right\},$$

$$\Psi(y, z) = \sum_{n=1}^{N_h \cdot N_U} \sum_{m=0}^{\infty} \left(\frac{2\pi n}{N_U \lambda_U} \right)^{2m} \left\{ \tilde{a}_n \cos \left(\frac{2\pi n z}{N_U \lambda_U} \right) + \tilde{b}_n \sin \left(\frac{2\pi n z}{N_U \lambda_U} \right) \right\} \cdot \frac{y^{2m+1}}{(2m+1)!}.$$

Components of the magnetic field $\vec{B} = \nabla \Psi$ can be calculated:

$$B_x = \frac{\partial \Psi(y, z)}{\partial x} = 0,$$

$$B_y = \frac{\partial \Psi(y, z)}{\partial y} = \sum_{n=1}^{N_h \cdot N_U} \left[\left\{ \tilde{a}_n \cos \left(\frac{2\pi n z}{N_U \lambda_U} \right) + \tilde{b}_n \sin \left(\frac{2\pi n z}{N_U \lambda_U} \right) \right\} \cdot \sum_{m=0}^{\infty} \left(\frac{2\pi n}{N_U \lambda_U} \right)^{2m} \frac{y^{2m}}{(2m)!} \right],$$

$$B_z = \frac{\partial \Psi(y, z)}{\partial z} = \sum_{n=1}^{N_h \cdot N_U} \left[\left\{ -\tilde{a}_n \sin \left(\frac{2\pi n z}{N_U \lambda_U} \right) + \tilde{b}_n \cos \left(\frac{2\pi n z}{N_U \lambda_U} \right) \right\} \cdot \sum_{m=0}^{\infty} \left(\frac{2\pi n}{N_U \lambda_U} \right)^{2m+1} \frac{y^{2m+1}}{(2m+1)!} \right].$$

LCLS-I Undulator field

3D field map generation

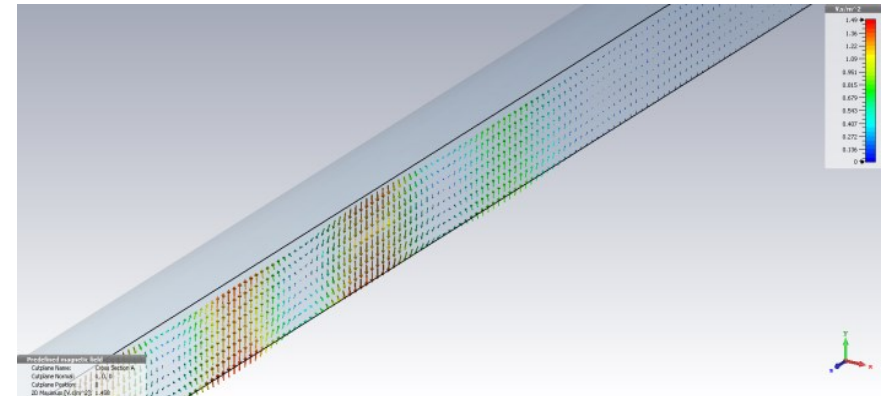
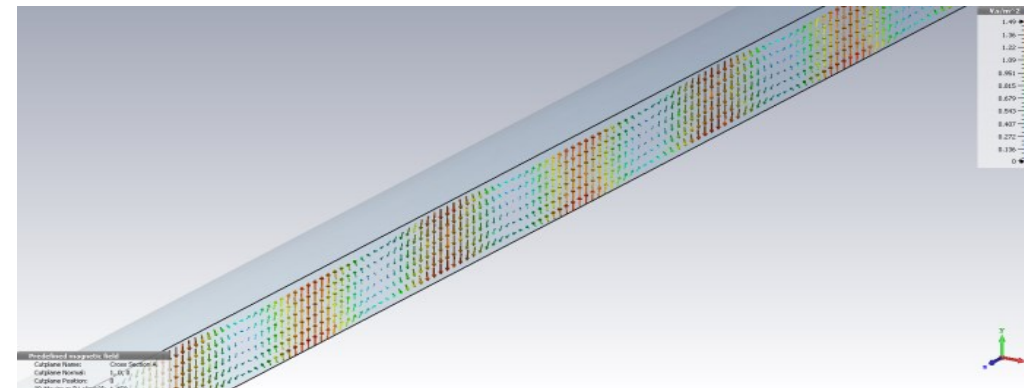
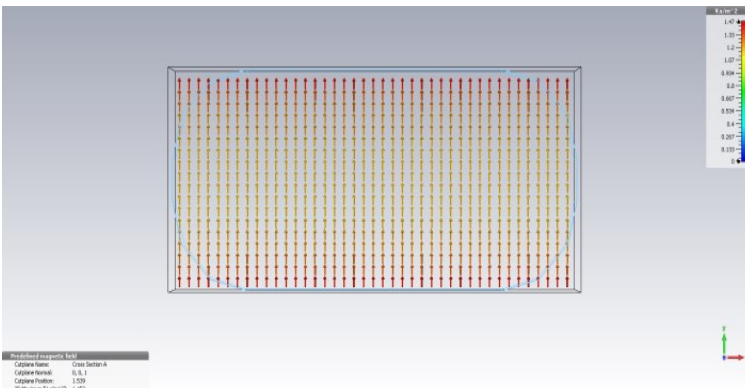
Utilizing

$$\sum_{m=0}^{\infty} \frac{\xi^{2m}}{(2m)!} = \cosh \xi, \sum_{m=0}^{\infty} \frac{\xi^{2m+1}}{(2m+1)!} = \sinh \xi,$$

Vertical and longitudinal components can be finally re-written:

$$B_y = \sum_{n=1}^{N_h \cdot N_U} [\{\tilde{a}_n \cos(k_n z) + \tilde{b}_n \sin(k_n z)\} \cdot \cosh(k_n y)],$$
$$B_z = \sum_{n=1}^{N_h \cdot N_U} [\{-\tilde{a}_n \sin(k_n z) + \tilde{b}_n \cos(k_n z)\} \cdot \sinh(k_n y)],$$

where $k_n = \frac{2\pi n}{N_U \lambda_U}$ is the wavenumber of the n -th Fourier harmonic.

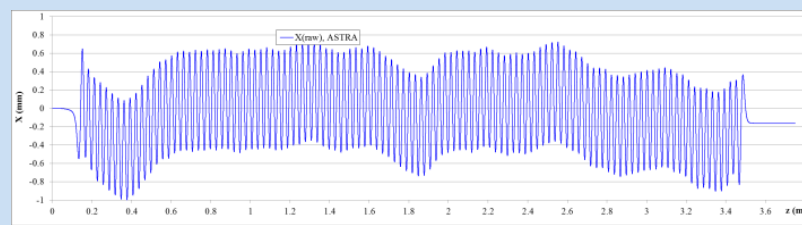


On-axis particle trajectory in the undulator

ASTRA reference particle and CST tracking

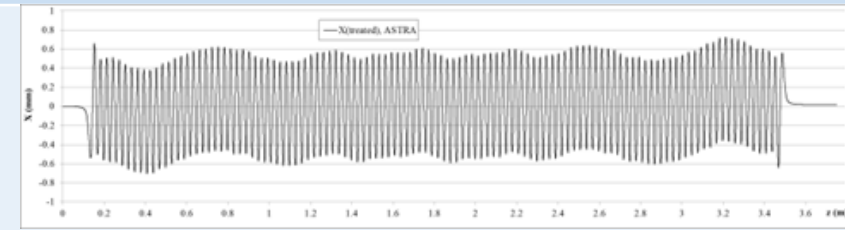
Undulator field profile
used for field map
generation

Raw measurements

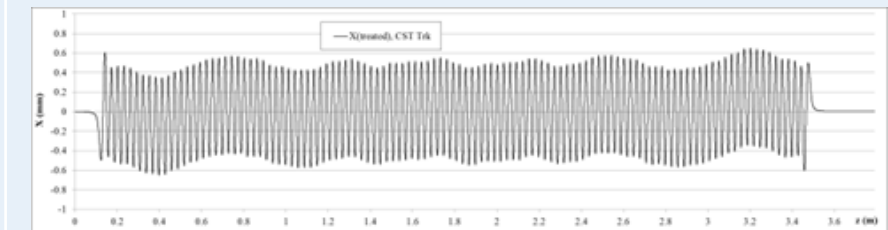
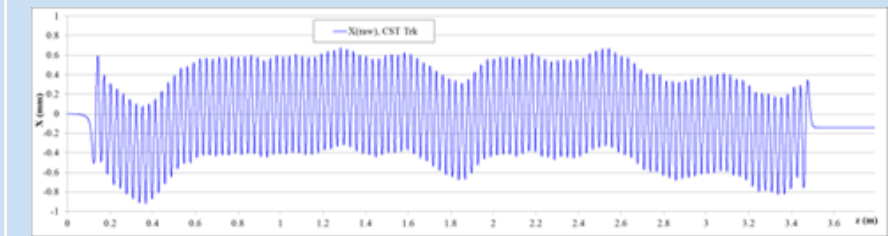


ASTRA with 3D field map

Improved profile



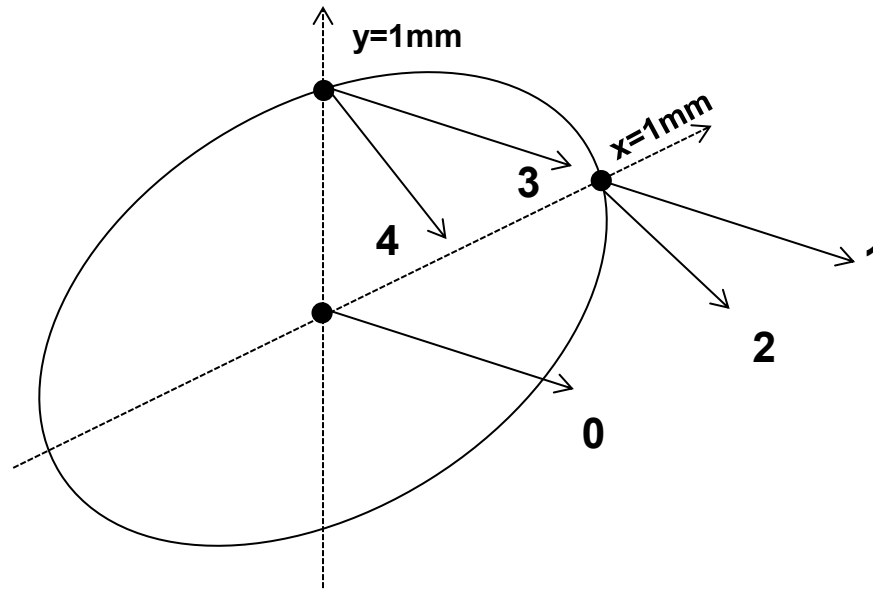
CST Particle Studio Trk



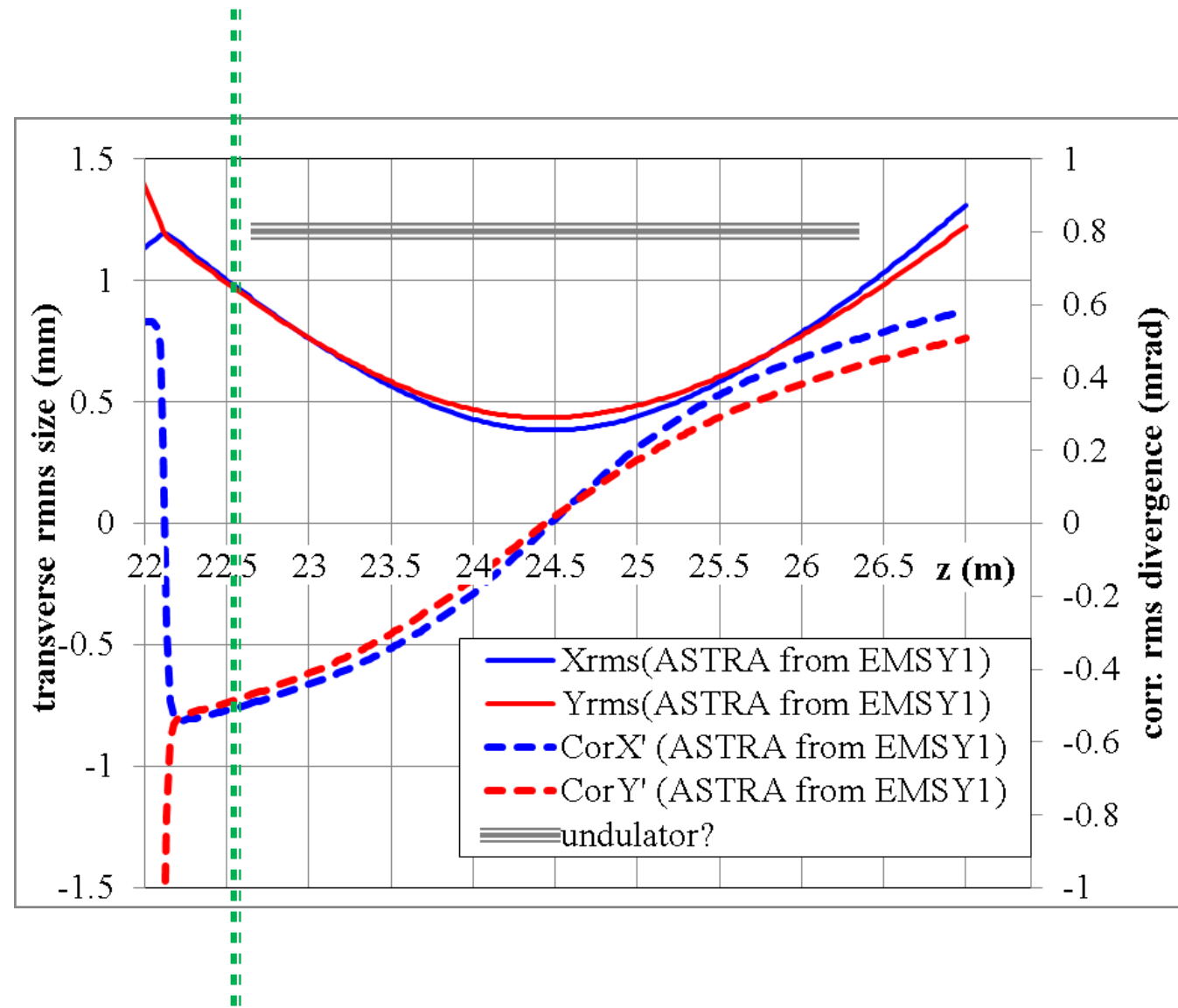
Vertical on-axis trajectory $\rightarrow y=0$

Off-axis particle trajectory in the undulator

ASTRA reference particle

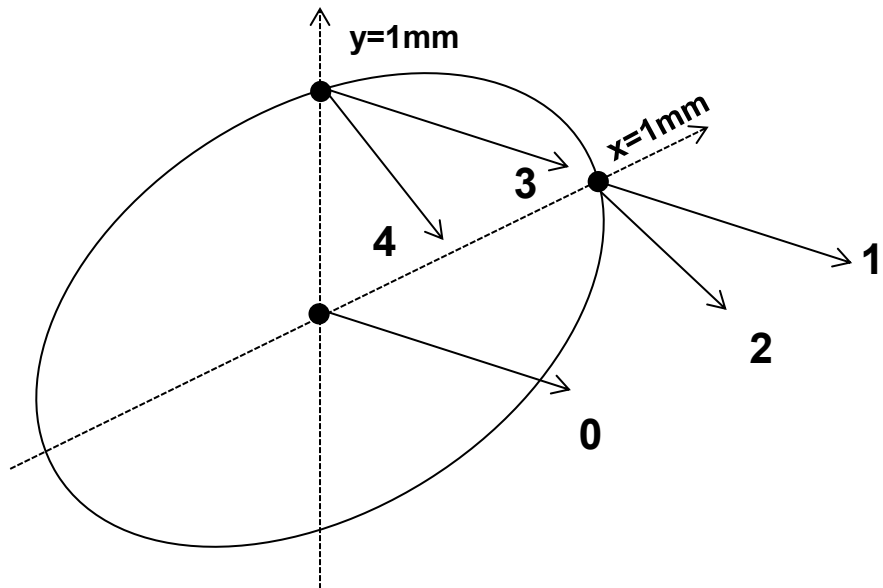


case	X(0), mm	X'(0), mrad	Y(0), mm	Y'(0), mrad
0	0	0	0	0
1	1	0	0	0
2	1	-0.5	0	0
3	0	0	1	0
4	0	0	1	-0.5
5	0.7	-0.35	0.7	-0.35

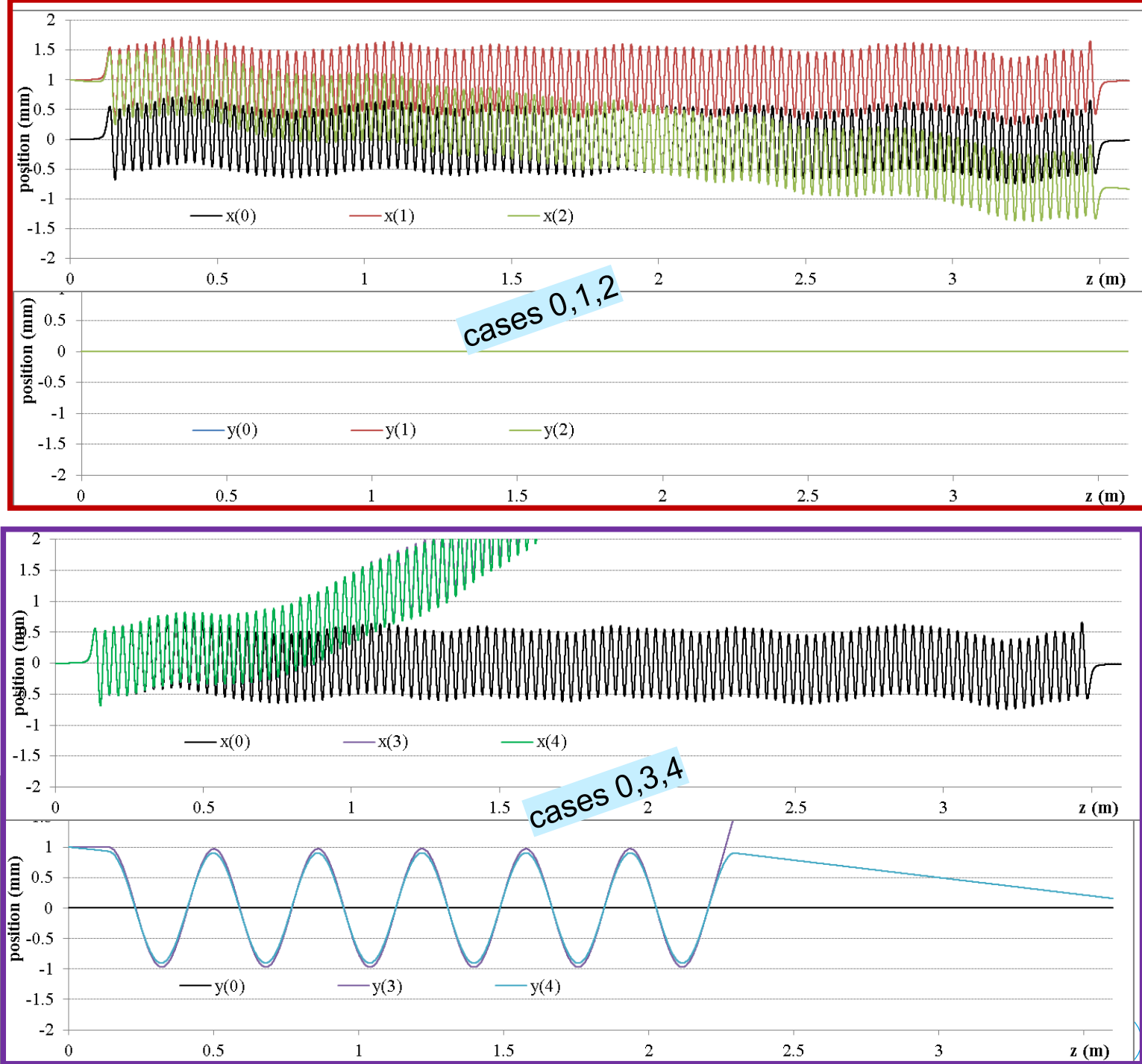


Off-axis particle trajectory in the undulator

ASTRA reference particle

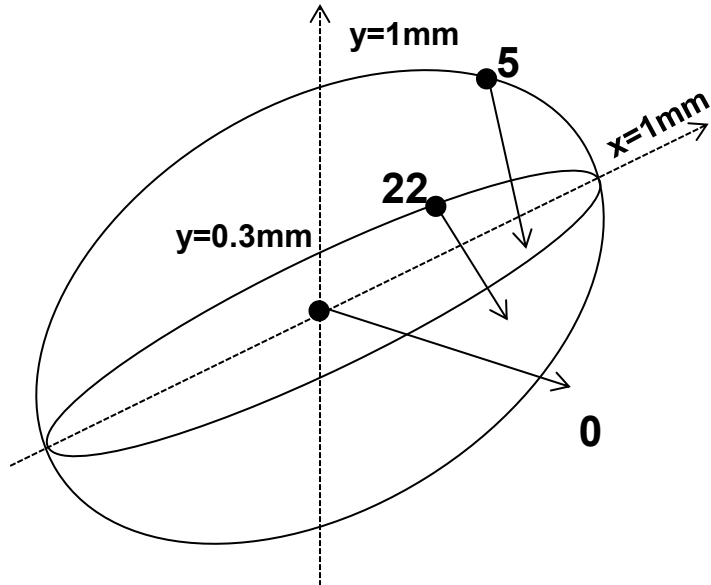


case	X(0), mm	X'(0), mrad	Y(0), mm	Y'(0), mrad
0	0	0	0	0
1	1	0	0	0
2	1	-0.5	0	0
3	0	0	1	0
4	0	0	1	-0.5
5	0.7	-0.35	0.7	-0.35

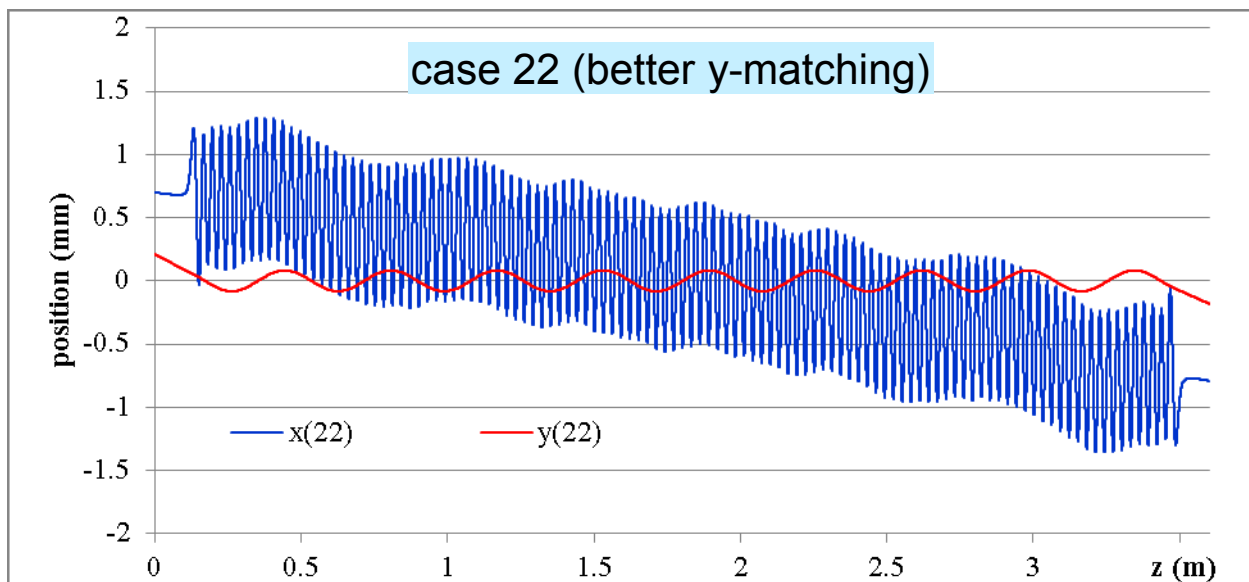
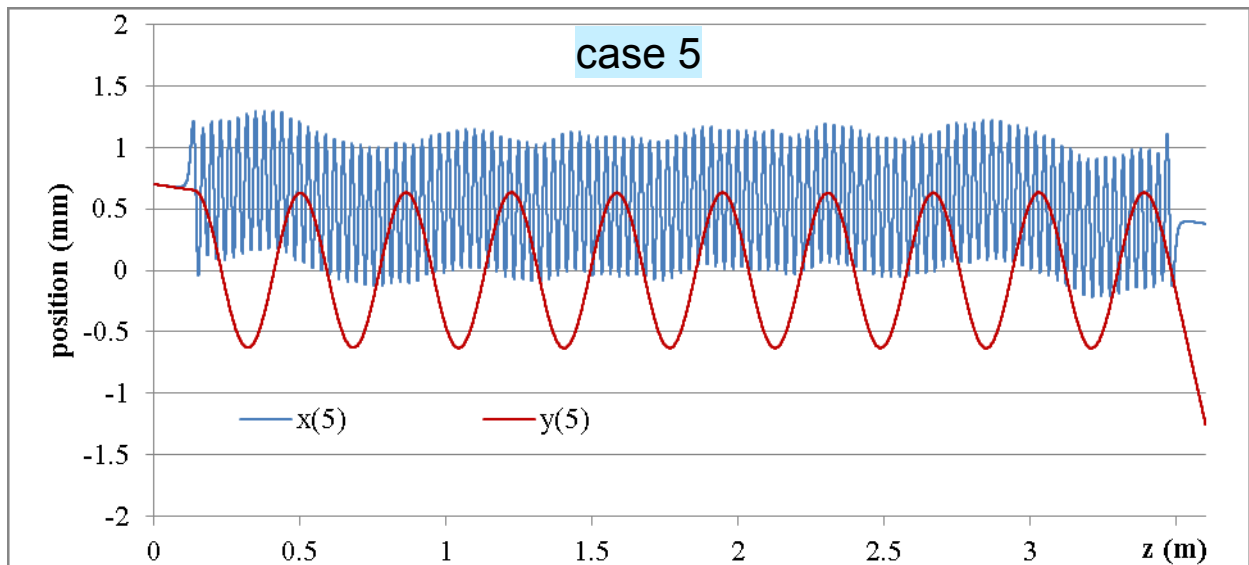


Off-axis particle trajectory in the undulator

ASTRA reference particle



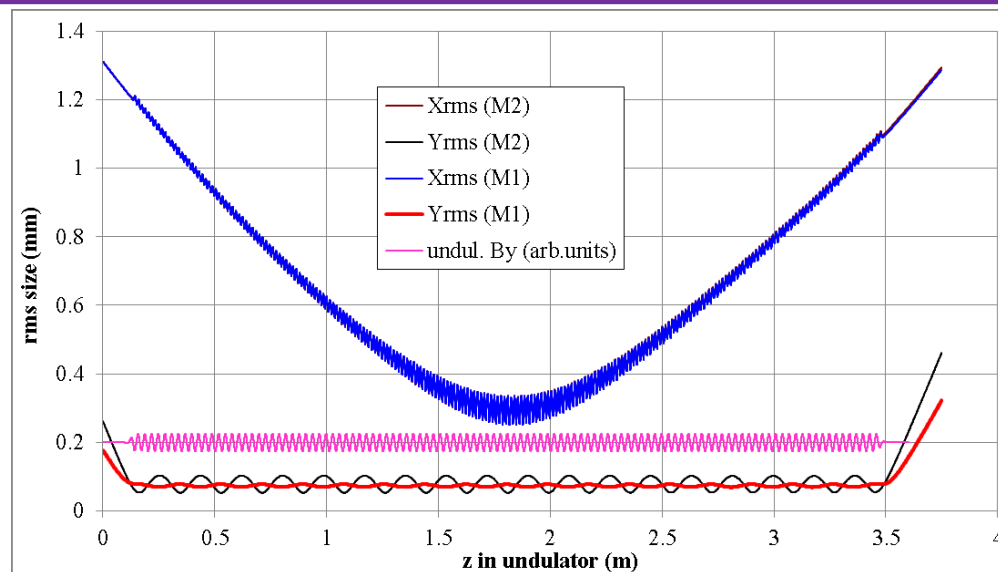
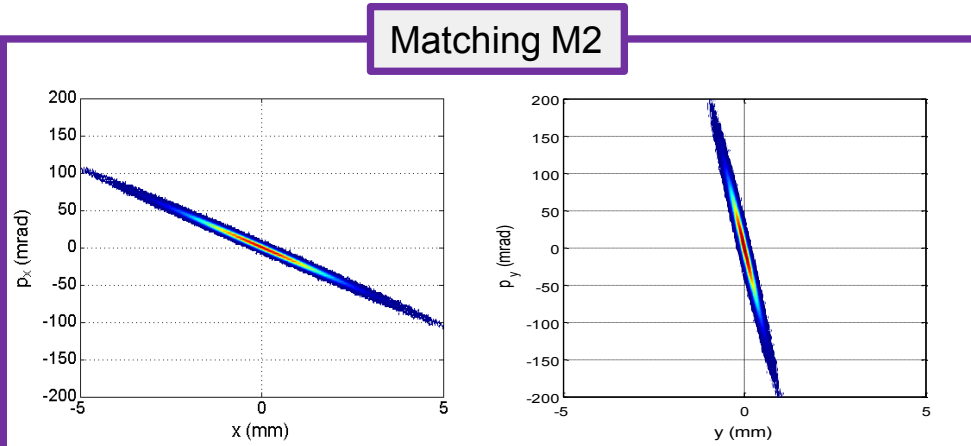
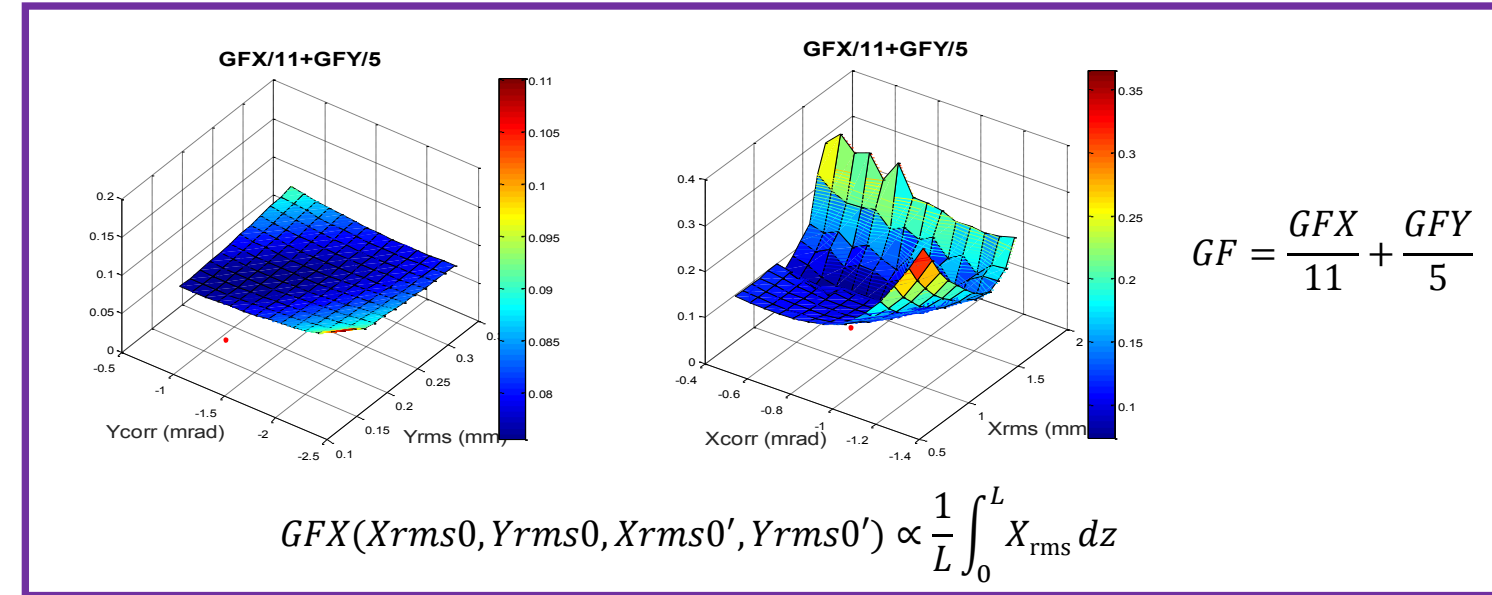
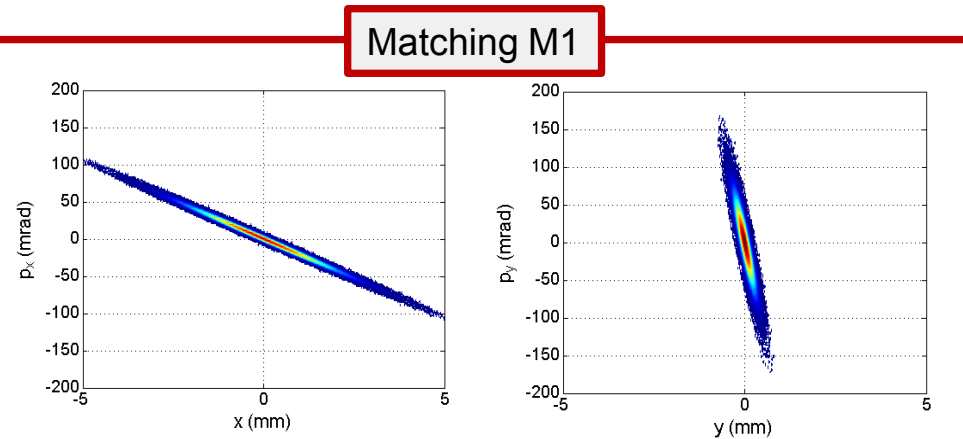
case	X(0), mm	X'(0), mrad	Y(0), mm	Y'(0), mrad
5	0.7	-0.35	0.7	-0.35
22	0.7	-0.35	0.21	-1.19



Beam matching into the undulator

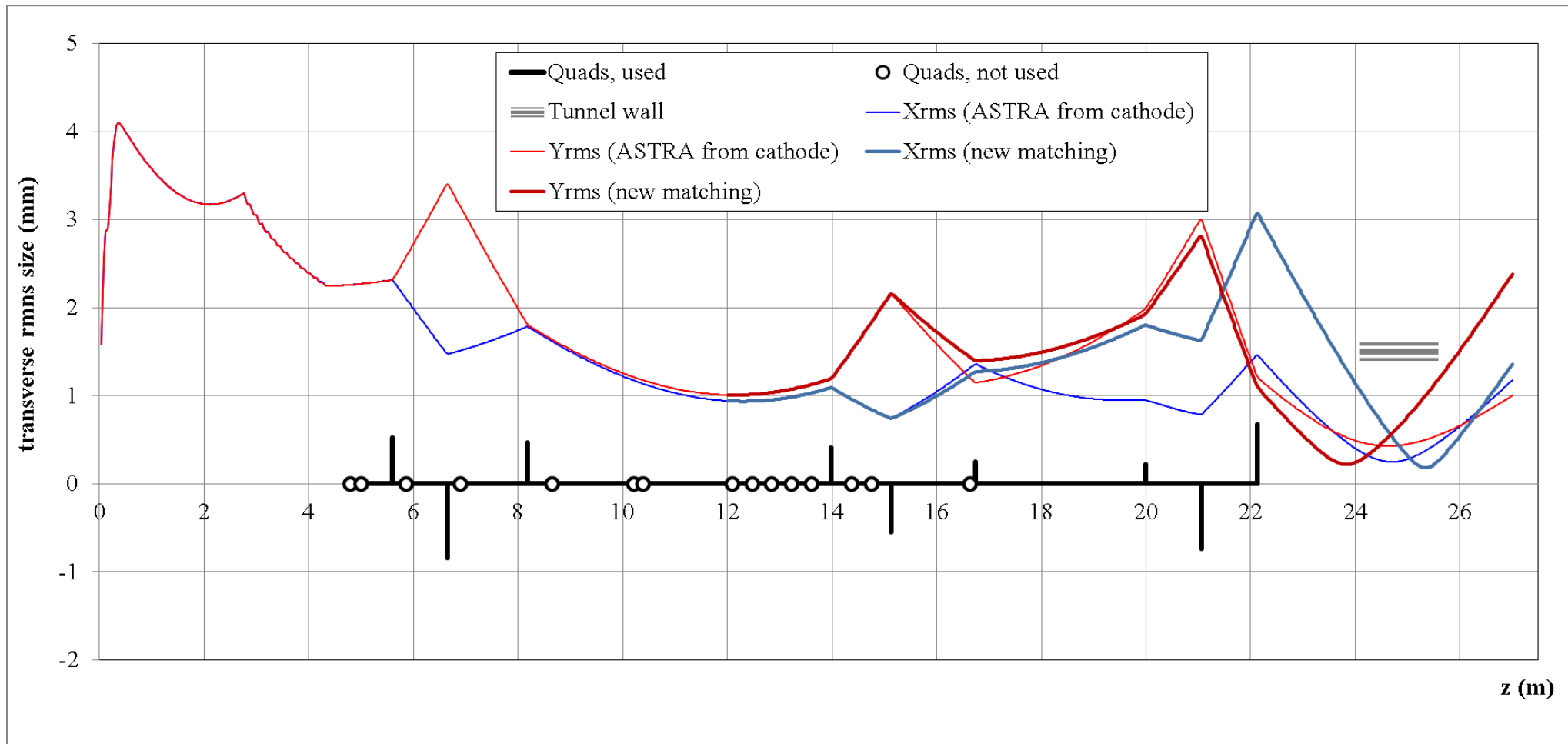
ASTRA simulations with space charge and 3D undulator field map

- “Ideal” (Gaussian-FT) beam



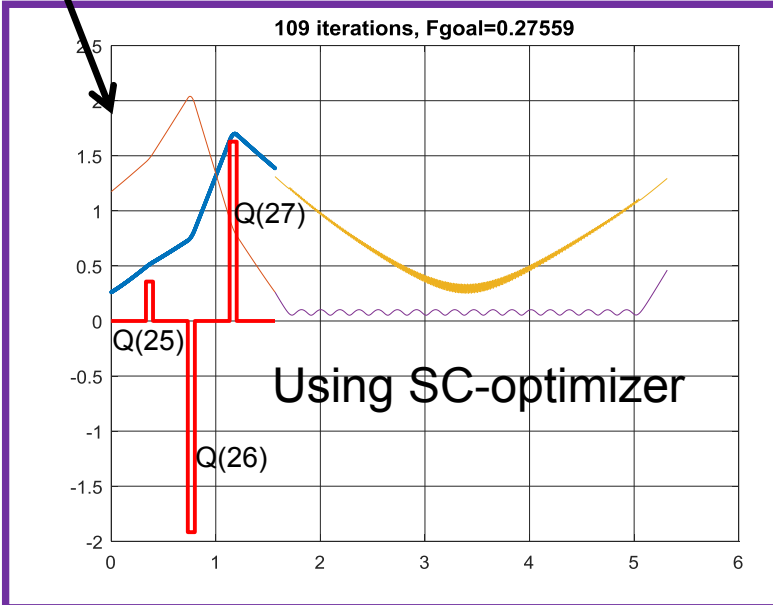
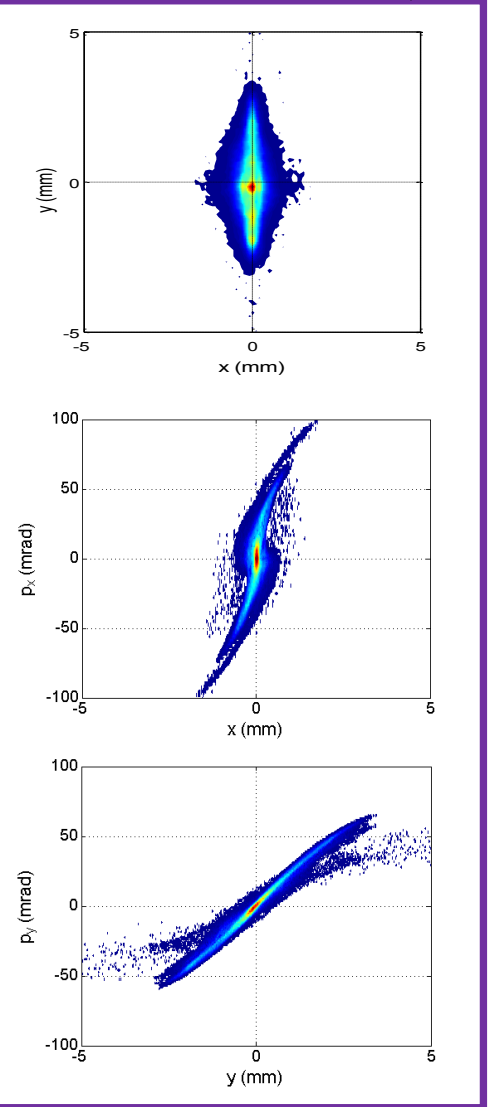
New transport / matching

Further “through the wall” + prepare for asymmetric matching into the undulator



Fine matching into the undulator

Starting with “beam at wall of the new tunnel” z=25.587m



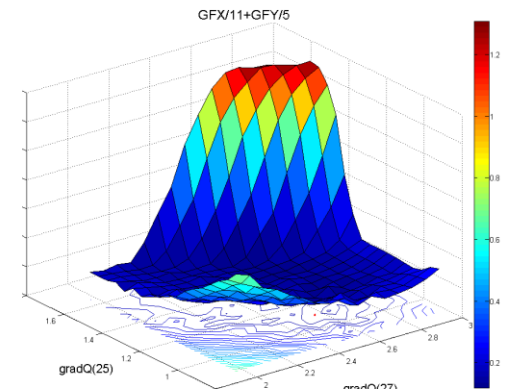
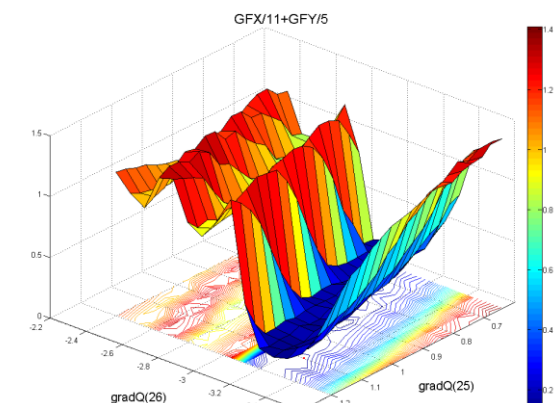
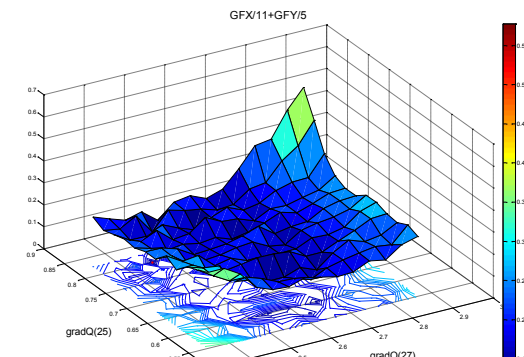
Quad	Z from wall	Z from cathode	Matching M1		Matching M2	
			T/m	A	T/m	A
Q(25)	0.3663	25.9533	1.107	~1.6	1.425	~2.1
Q(26)	0.7663	26.3533	-3.277	~-4.8	-3.277	~-4.8
Q(27)	1.1663	26.7533	2.564	~3.8	2.564	~3.8

$$GFX(X_{\text{rms}0}, Y_{\text{rms}0}, X_{\text{rms}0'}, Y_{\text{rms}0'}) \propto \frac{1}{L} \int_0^L X_{\text{rms}} dz$$

$$GFY(X_{\text{rms}0}, Y_{\text{rms}0}, X_{\text{rms}0'}, Y_{\text{rms}0'}) \propto \frac{1}{L} \int_0^L Y_{\text{rms}} dz$$

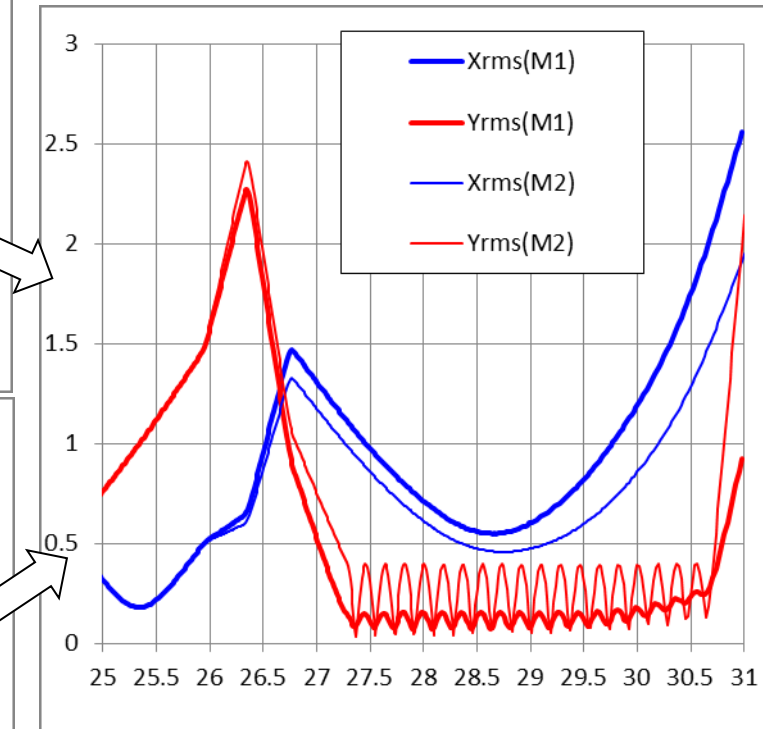
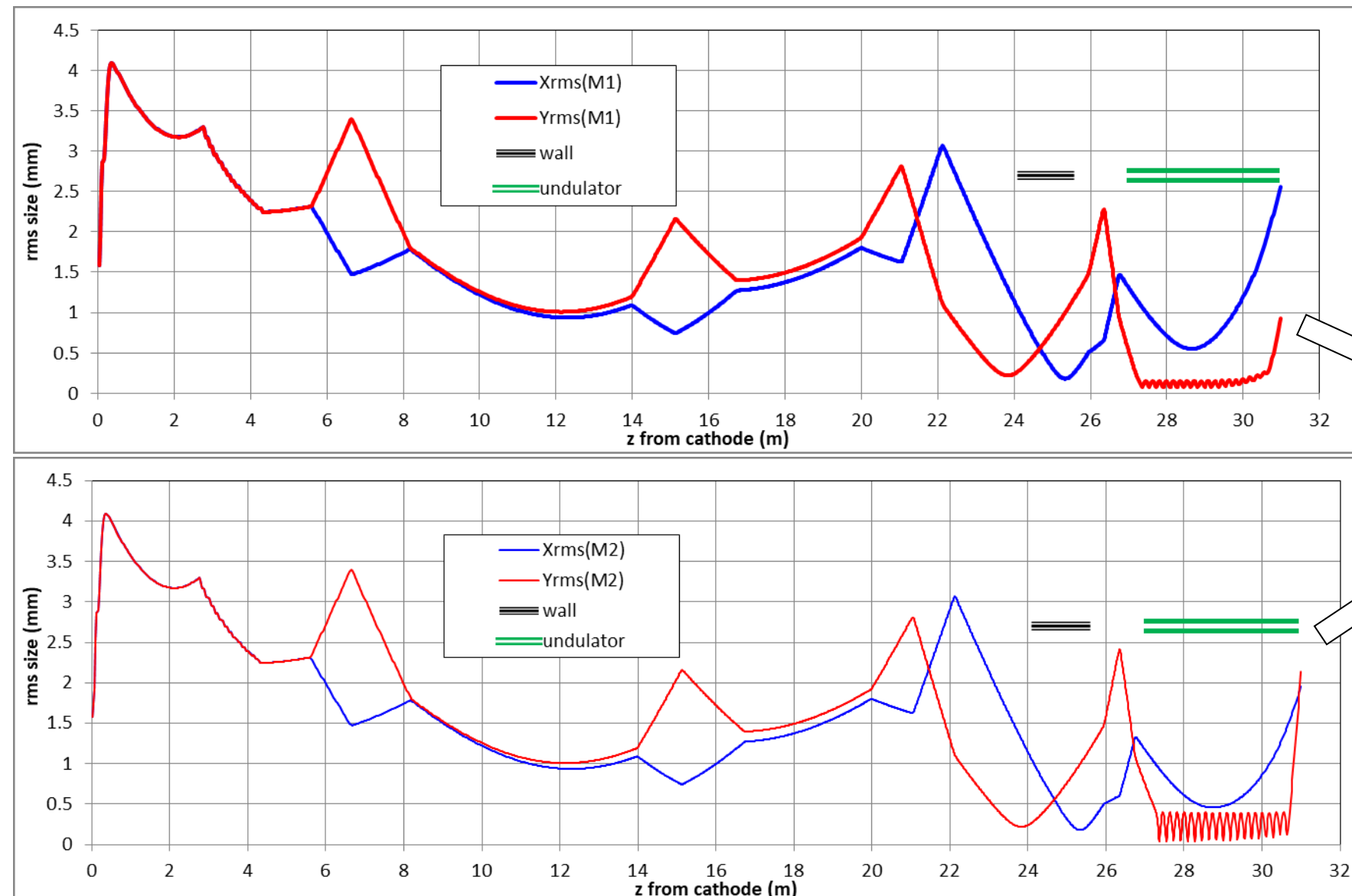
$$GF = \frac{GFX}{11} + \frac{GFY}{5}$$

Using ASTRA



Electron beam transport for LCLS-I undulator option at PITZ

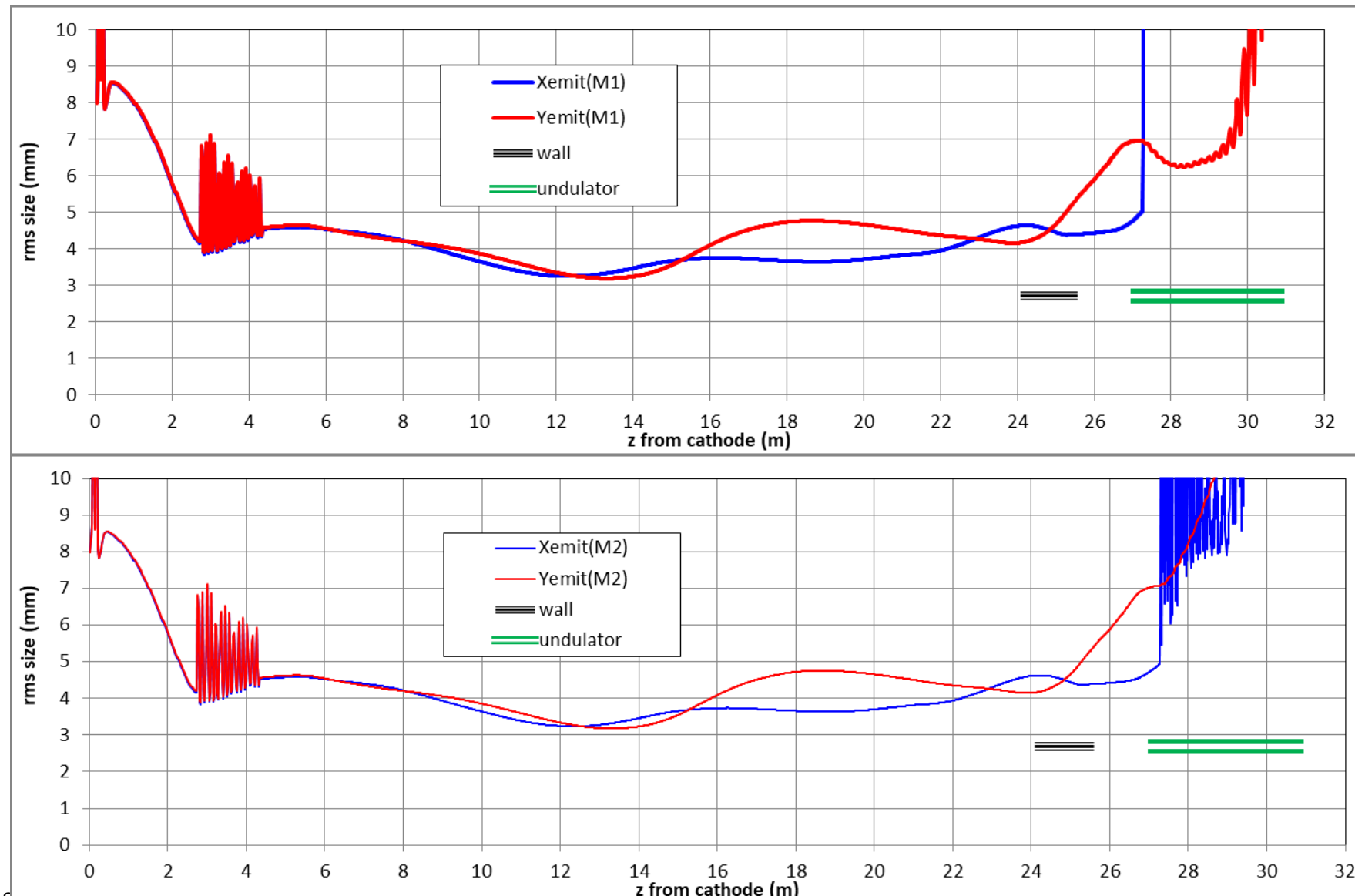
2 solution s (M1 and M2) for the matching into the undulator → beam size



NB: 6pC of 4nC lost at the end of the undulator... 😞

Electron beam transport for LCLS-I undulator option at PITZ

2 solution s (M1 and M2)for the matching into the undulator → emittance



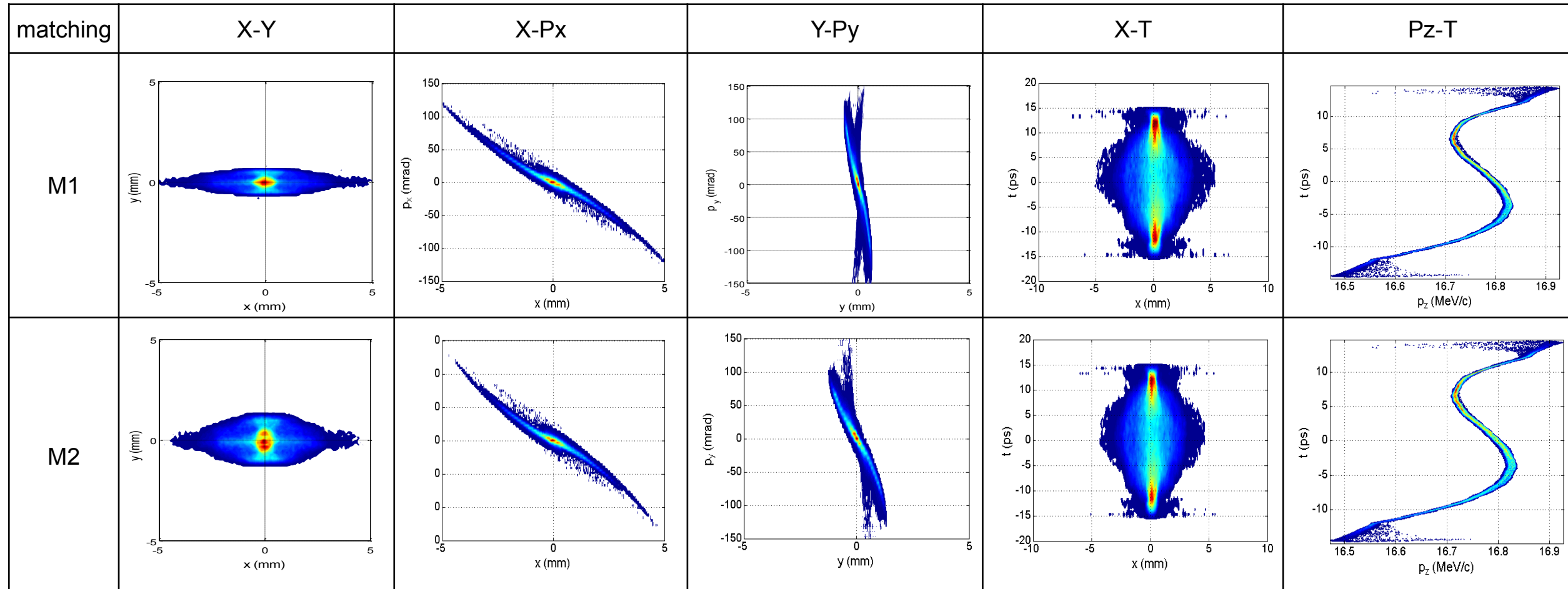
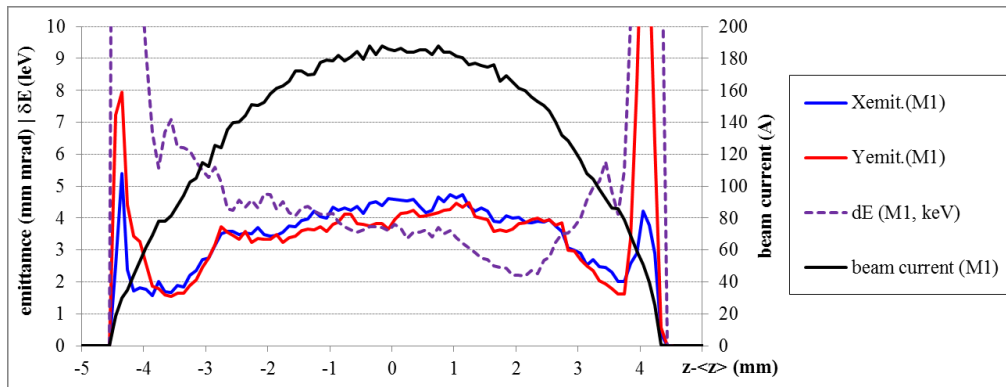
CST Particle Studio Simulations

More correct space charge estimations + vacuum chamber impact

- Still on-going...

Beam at undulator entrance

ASTRA monitors at z=27.15m



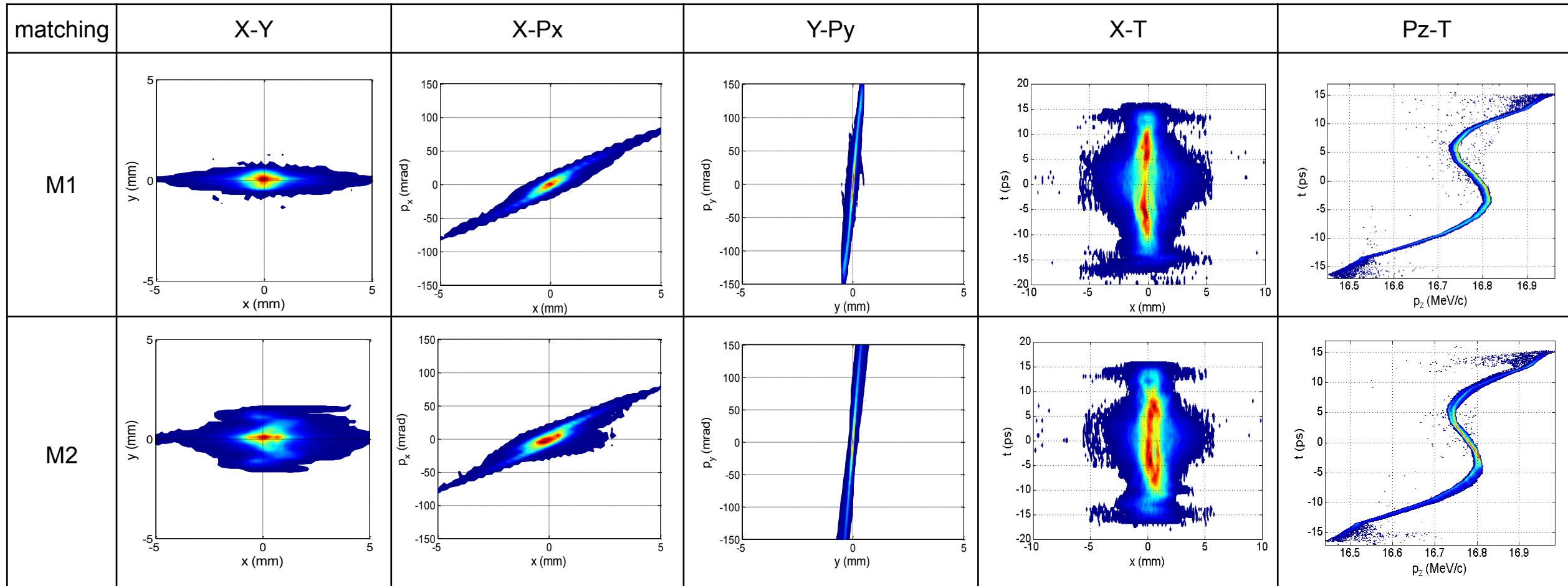
GENESIS1.3 Simulations

ASTRA at 27.15m → GENESIS1.3

- See slides from Prach

Beam at undulator exit

ASTRA monitors at z=30.7m



Conclusions

Star-to-End simulations for the proof-of-principle experiment for SASE THz FEL at PITZ using LCLS-I undulator

- PITZ Setup:

- Gun: 60MV/m, 0deg
- Photocathode laser: Ø5mm, 21.5ps FWHM, 4nC
- CDS booster setup: 12.6MV/m, -24deg → 16.7MeV/c + min dE@~undulator
- Main solenoid: MaxB(1)=-0.21285T (~365A) → ε_{xy} (EMSY1)~4.6 mm mrad
- Transport: 3 quad. triplets → transport through the tunnel wall (1.5m)
- Transport: +1 quad triplet to match into undulator

- Undulator field:

- Based on measured profile $B_y(z,0,0)$
- Treated (improved) profile to minimize field integrals
- 3D field map reconstructed → CST and ASTRA

- Tracking beam through the undulator:

- On-axis reference particle: CST Trk ↔ ASTRA with 3D field map
- Off-axis reference particle in ASTRA to find initial guess for matching
- 4nC beam by ASTRA (with space charge*) → M1 and M2 found

- ...

PITHz: THz proof-of-principle experiments at PITZ (LCLS-I-und)

Current status (10.09.2018) and outlook

Open questions

- Refine (improve) preliminary optimum solution:
 - Matching after the wall and between U1 and U2 (cross-check with PIC solver)
 - Modeling and optimization of the collimator section
 - ...
- Realistic PC laser parameters $\varnothing 3\text{-}4\text{mm}$, other temporal profiles, core+halo (using experimental data)
- Scale / re-optimize setup for $\lambda_{\text{rad}}=50\text{-}60\mu\text{m}$
- Prepare experimental program to check 4nC electron beam transport
- Modeling of the THz measurement setup (together with FLASH, N.Stojanovic?)
- Waveguide effects in the THz SASE FEL (together with G.Geloni?)
- Undulator radiation from short bunches
- Seeding option simulations (modulated PC laser – based on input from IAP)
- BC design (pool of available magnets?)
- 2nd CDS booster?
- ...

Expected results

- PITZ layout update: new quads, steerers, collimator(s) and diagnostics → prepared for technical design
- Realistic modeling of high charge beam dynamics in the PITZ beamline
- Prepared setups for $\lambda_{\text{rad}}=50\text{-}100\mu\text{m}$ for experimental tests
- ...

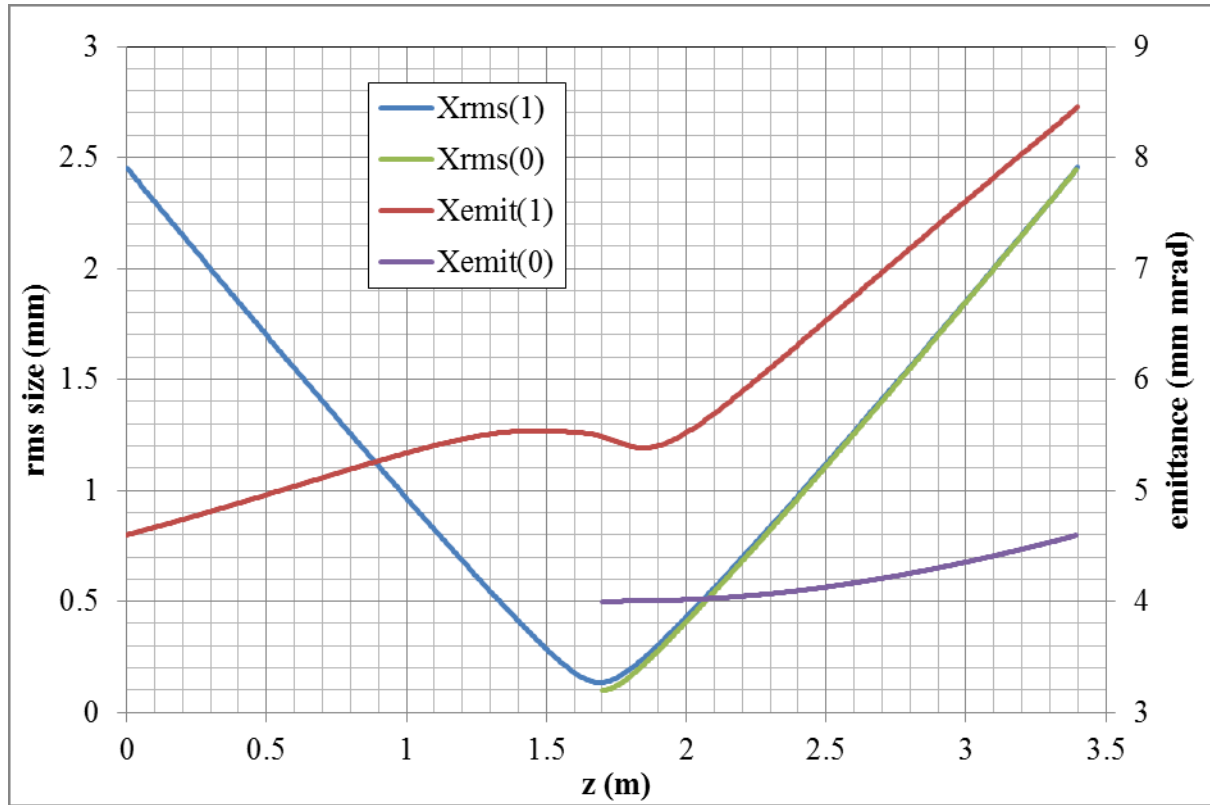
Mini-workshop on proof-of-principle SASE THz FEL at PITZ

½ - 1 day in the 1st ½ of October

- PITZ accelerator (general layout and parameters)
- Preliminary simulations for THz options at PITZ, experimental results on THz CTR/CDR
- Proposals for proof-of-principle experiments using LCLS-I undulator(s)
- Start-to-end simulations for the proof-of-principle experiments (SASE THz FEL)
- Possible critical problems (real beam transport, wakefield, waveguide regime, etc.)
- Experimental program on the electron beam characterization (4nC emittance and transport)
- PITZ layout modification for LCLS-I undulator installations
- Required electron beam diagnostics
- Machine protection system (BLM, collimator, etc.)
- Required THz diagnostics
- Other options with LCLS-I undulator (undulator radiation with short bunches, seeding, etc.) and required components (e.g., bunch compressor)
- Technical issues (construction, electronics, controls)
- Possible timeline

Estimations on beam size in a drift

0.1 mm rms waist → not optimum



Electron beam transport for LCLS-I undulator option at PITZ

2 solution s (M1 and M2)for the matching into the undulator → beta functions

